Quaternary Science Reviews 159 (2017) 15–34

Contents lists available at ScienceDirect

Quaternary Science Reviews

journal homepage: www.elsevier.com/locate/quascirev

# Timing and process of river and lake terrace formation in the Kyrgyz Tien Shan

Reed J. Burgette [a, b, *], Ray J. Weldon II [a], Kanatbek Ye. Abdrakhmatov [c], Cholponbek Ormukov [c, 1], Lewis A. Owen [d], Stephen C. Thompson [a, e]

[a] University of Oregon, Department of Geological Sciences, 1272 University of Oregon, Eugene, OR 97403, USA
[b] New Mexico State University, Department of Geological Sciences, PO Box 30001, MSC 3AB, Las Cruces NM 88003, USA
[c] Kyrgyz Institute of Seismology, 52/1, Asanbai Microdistrict, Bishkek 720060, Kyrgyz Republic
[d] Department of Geology, University of Cincinnati, Cincinnati, OH 45221, USA
[e] Lettis Consultants International, 1981 N Broadway, Suite 330, Walnut Creek, CA 94596, USA

ARTICLE INFO

*Article history:*
Received 29 March 2016
Received in revised form
9 December 2016
Accepted 4 January 2017

*Keywords:*
Terraces
Aggradation
Incision
Issyk-Kul
Tien Shan
Lake level
Quaternary
Central Asia

ABSTRACT

Well-preserved flights of river and lake terraces traverse an actively deforming rangefront, and form a link between glaciated mountains and a large intermontane lake in the Issyk-Kul basin of the Kyrgyz Tien Shan. We investigated the history and geometry of these lake and river terraces using geologic mapping, surveying, and radiocarbon and terrestrial cosmogenic nuclide dating. A prominent late Pleistocene highstand of the lake occurred over at least the period of 43–25 ka, followed by a period of deep regression and subsequent rise of the lake to the modern sill level in the late Holocene. Major aggradation of the most prominent latest Quaternary river terrace along the Ak-Terek and Barskaun rivers likely started at ~70–60 ka, coincident to the local last glacial maximum in this region. In contrast to some models of aggradation and incision, the rivers appear to have stayed near the top of the fill for >20 ka, incising subtly below the top of this fill by ~37 ka, locally. Deep incision likely did not occur until the peak deglaciation in the latest Pleistocene. Older dated terrace surfaces are consistent with one major terrace-forming event per glacial, constant deformation and incision rates, and typical fluvial gradients lower than the modern incising streams. The dating confirms regional terrace correlations for the most prominent late Quaternary terraces, but correlating higher terraces is complicated by spatially varying uplift rates and preferential terrace preservation between basins in the Tien Shan.


## 1. Introduction

The Tien Shan is one of the most active mountain belts on Earth and provides a natural laboratory to study landscape evolution in an intracontinental setting. Active contractional deformation produces variations in rock uplift rate along river systems, and flights of river terraces and alluvial fans are preserved along many river systems, often connecting glacial and lacustrine landforms that provide proxies for climate change (e.g., Aleshinskaya et al., 1971; Thompson et al., 2002; Koppes et al., 2008). This setting provides an excellent place to examine the timing and process of river terrace formation related to climatic and base-level variations.

A river terrace forms when a river cuts through its bed following a period of relative vertical stability or aggradation in response to climatic and tectonic forcings (e.g., Bull, 1991). Rapid, large magnitude variations in base-level caused by sea or lake level changes exert an important control on rivers that drain into oceans or large lakes (Merritts et al., 1994; Pazzaglia and Brandon, 2001). Temporal changes in base-level from tectonic fluctuations also provide a potential means of driving punctuated incision or aggradation along a river. However, most observations of major terrace forming periods align with major Quaternary climate fluctuations, even in areas of tectonic deformation (e.g., Molnar et al., 1994; Bridgland and Westaway, 2008).

The balance between sediment supply and stream power, which

* Corresponding author. New Mexico State University, Department of Geological Sciences, PO Box 30001, MSC 3AB, Las Cruces NM 88003, USA.
*E-mail addresses:* burgette@nmsu.edu (R.J. Burgette), ray@uoregon.edu (R.J. Weldon), kanab53@yandex.com (K.Ye. Abdrakhmatov), cholponbek76@yahoo.com (C. Ormukov), lewis.owen@uc.edu (L.A. Owen), thompson@lettisci.com (S.C. Thompson).
[1] Present Address: Central-Asian Institute for Applied Geosciences, Timur Frunze Rd.73/2, Bishkek 720027, Kyrgyz Republic.

http://dx.doi.org/10.1016/j.quascirev.2017.01.003
0277-3791/

is thought to be the primary control on terrace formation, is dependent in a complex way on climatic factors that have varied temporally and spatially over the late Quaternary (Bull, 1991; Merritts et al., 1994; Pazzaglia and Brandon, 2001; Hancock and Anderson, 2002). For example, shifts to greater precipitation have been inferred to drive a range of outcomes in different landscapes. In some settings, increases in precipitation have driven aggradation by enhancing rates of mass wasting from hillslopes into the fluvial network (e.g., Bull, 1991; Personius et al., 1993). In other landscapes, increased precipitation has caused incision through previously aggraded sediments to create river terraces and incised alluvial fans (e.g., Bull, 1991; Porter et al., 1992; Molnar et al., 1994; Pan et al., 2003; Lu et al., 2010).

In this study we characterize the geometry, stratigraphic relationships, and ages of river and lake terraces in the southern Issyk-Kul basin of the Kyrgyz Tien Shan (Fig. 1). The rivers of the southern Issyk-Kul basin traverse active reverse faults and folds with varying degrees and senses of offset. These rivers drain into Issyk-Kul (Issyk means warm and Kul means lake in Kyrgyz), which is the fifth deepest lake in the world and eleventh largest by volume (Herdendorf, 1990), and has experienced major fluctuations in level and extent throughout the Quaternary. We assess the contributions of base-level and climatic factors in driving terrace formation and incision in the region through synthesizing the timing of southern Issyk-Kul terraces with historic and emerging chronologies of the terrace formation and glaciation from elsewhere in the Tien Shan region. We conclude by highlighting the implications of these remarkably well-preserved river and lacustrine terraces of the Tien Shan for neotectonic and geomorphic studies in the region and elsewhere.

### 1.1. Study area

The Tien Shan is an east-trending high mountain belt in the interior of Eurasia (Fig. 1). The mountains are forming due to distributed reverse faulting and folding in the Eurasian lithosphere that accommodates convergence between India and Eurasia (e.g., Molnar and Tapponnier, 1975). The Tien Shan is the most active locus of late Cenozoic shortening north of the Himalayan frontal thrust faults, and active deformation is distributed across several major fault systems within and at the edges of the belt (Abdrakhmatov et al., 1996; Thompson et al., 2002).

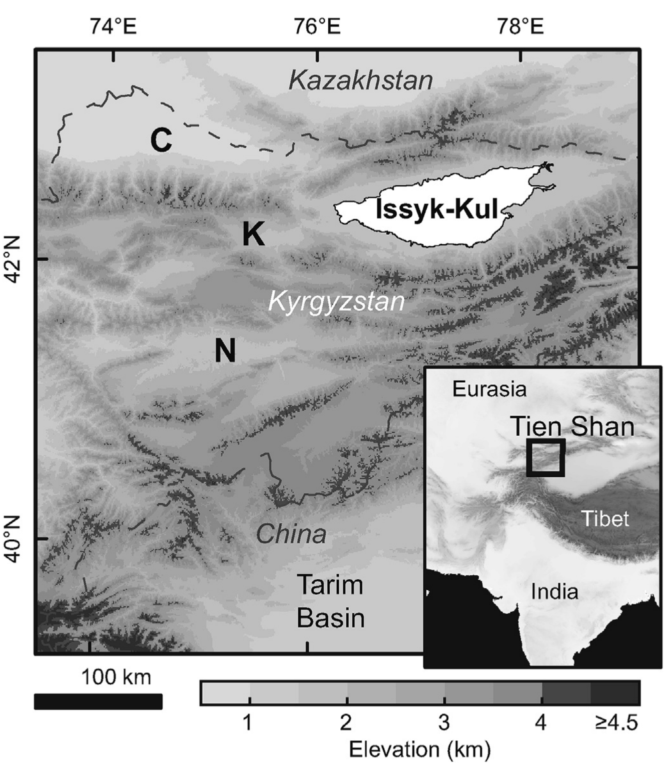


**Fig. 1.** Tien Shan Range, central Asia. Inset gives position of the Kyrgyz Tien Shan in the larger India-Asia collision. Other basins west of Issyk-Kul in the central Tien Shan with dated terraces (Thompson et al., 2002): C, Chu; K, Kochkor; N, Naryn.

In a regional sense, the Tien Shan represents a reactivated area of Paleozoic deformation. Following the Paleozoic orogenies, the region was planed off to a low-relief surface (Chediya, 1986). Late Cenozoic deformation has resulted in this surface being warped across a series of mountain ranges cored by crystalline basement and previously deformed Paleozoic sedimentary and metamorphic rocks. The intervening basins have been filled by thick sections of syntectonic sediment (e.g., Abdrakhmatov et al., 2001).

One of the largest basins within the Kyrgyz portion of the Tien Shan is the Issyk-Kul basin, named after the lake, Issyk-Kul, which occupies much of the basin (Fig. 2). Modern Issyk-Kul is internally drained, with a surface area of 6200 km$^2$, a maximum depth of 668 m, and a surface elevation of ~1607 m above mean sea level (amsl). The Issyk-Kul basin is bounded to the south by the actively growing Terskey Ala-Tau Range, which includes numerous glaciated peaks that rise above 4000 m amsl (Fig. 2). Rivers in southwestern Issyk-Kul traverse south-vergent structures, which form uphill-facing topography and often show signs of progressive stream capture. The rivers of southeastern Issyk-Kul cut through a large north-vergent fold limb that has been tilting the land surface up to the south over the last few million years (Burgette, 2008).

### 1.2. Previous Kyrgyz Tien Shan river terrace correlation and dating

Quaternary landforms and associated sedimentary deposits in the Tien Shan have been studied extensively by Soviet and Kyrgyz Quaternary scientists (e.g., Grigorienko, 1970; Grigina and Fortuna, 1981; Trofimov, 1990) and correlated through a relative dating scheme (Fig. 3). This Quaternary framework relies on morphologic similarity, stratigraphic correlation, paleontology, correlation with global climatic change, and a few radiometric ages (e.g., Grigorienko, 1970). The morphostratigraphic approach, assuming landforms can be appropriately correlated from one area to another, offers a first-order method for understanding patterns of paleohydrology and tectonics over extensive areas.

In the Kyrgyz Tien Shan, the Quaternary is divided into four primary divisions: from oldest to youngest these are $Q_I$ to $Q_{IV}$ (Grigorienko, 1970). $Q_{IV}$ is generally correlative with the Holocene (Melnikova, 1986). $Q_{III}$, $Q_{II}$, and $Q_I$ have been thought to represent climatic cycles in the late to middle Pleistocene (e.g. Trofimov, 1990). In many areas of the Tien Shan, geomorphic surfaces naturally lend themselves to classification in broad divisions, as sets of terraces are often grouped in elevation and are separated by larger elevation differences. Terraces within a group are subdivided with superscript Arabic numbers, again with lower numbers being older (Grigorienko, 1970). For example, the second oldest terrace in the $Q_{III}$ group is called $Q_{III}^2$. For flights of terraces that include more terraces than the regional pattern, we use decimals, such as $Q_{III}^{1.5}$, to maintain the correlation for the most prominent terraces in the regional scheme.

Based on our observations and guided by earlier literature, $Q_{IV}$ terraces, where present, occur as narrow cut surfaces on older fill deposits or as strath terraces in the hanging walls of the most active faults (Fig. 3). A single $Q_{IV}^1$ terrace is most common, but multiple $Q_{IV}$ terraces can be preserved in areas with high uplift rates.

The $Q_{III}$ terraces are the most prominent terraces associated with the modern rivers. The $Q_{III}^2$ terrace is generally broad and the

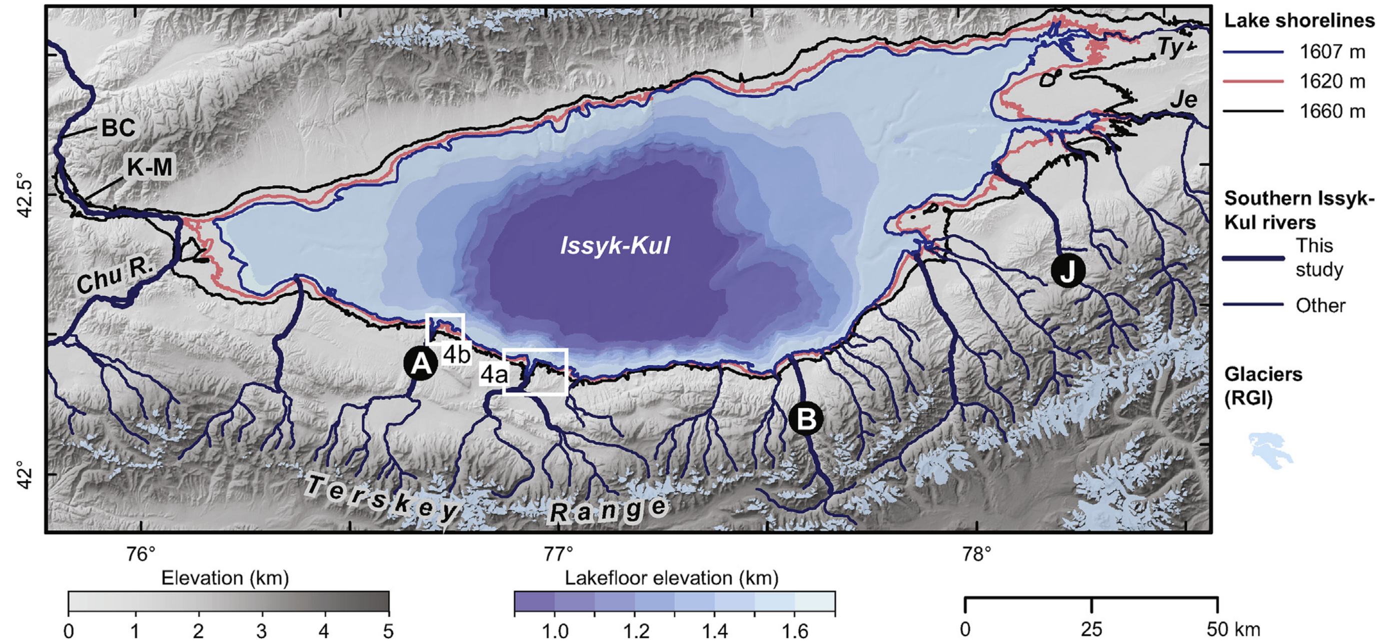


**Fig. 2.** Map of the Issyk-Kul basin, showing major rivers draining north out of the Terskey Range into Lake Issyk-Kul. Red and black lines show approximate levels of major lake highstands of Issyk-Kul in the late Holocene and late Pleistocene, respectively. Lake bathymetry (km amsl) is from De Batist et al. (2002). The six major rivers studied in Burgette (2008) are highlighted in bold and the three presented here are indicated: A, Ak-Terek; B, Barskaun; and J, Jety Oguz. Other features referenced in text: BC, Boam canyon; K-M, Kok-Moynok basin; Ty, Tyoup River; and Je, Jergalan River. Glacier extents are from the Randolph Glacier Inventory (Arendt et al., 2015). (For interpretation of the references to colour in this figure legend, the reader is referred to the web version of this article.)

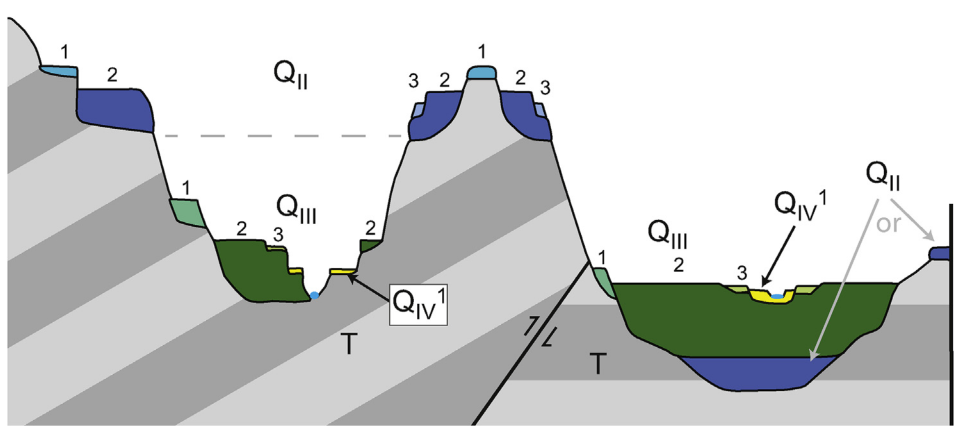


**Fig. 3.** Schematic section showing the Soviet morphostratigraphic naming system for late Quaternary river terraces in the Kyrgyz Tien Shan (after Grigorienko, 1970 and our observations). Blue and green polygons labeled with Roman and Arabic numbers show alluvial terrace gravel deposited on late Cenozoic rock (T). See text for details. Where relative subsidence rates are rapid on downthrown blocks, older terraces may be progressively buried (e.g. $Q_{II}$ on right side). (For interpretation of the references to colour in this figure legend, the reader is referred to the web version of this article.)

best developed. $Q_{III}^2$ terraces have thick fill deposits except for where rivers traverse areas of rapid incision associated with active structures (Fig. 3). Identification of $Q_{III}^2$ is generally a key step in making terrace correlations between rivers and basins. There is often a $Q_{III}^3$ cut terrace developed below the top of the $Q_{III}^2$ fill. Narrow strath or fill $Q_{III}^1$ terraces are commonly set into the canyon walls above $Q_{III}^2$, but well below $Q_{II}$ surfaces. In areas of relatively high incision rate, there are often multiple terraces with $Q_{III}^1$ geomorphic characteristics between $Q_{III}^2$ and $Q_{II}$.

$Q_{II}$ terraces are the oldest commonly preserved geomorphic surfaces, forming an extensive cap on the Tertiary sedimentary rock (Fig. 3). The highest levels of the $Q_{II}$ terraces do not appear localized with the modern canyons, but form broad bajada or pediment-like surfaces spanning multiple drainages. $Q_{II}^2$ is the most prominent $Q_{II}$ terrace, and is usually characterized by a fill morphology. Higher discontinuous $Q_{II}^1$ surfaces are preserved in places, and slightly inset $Q_{II}^3$ terraces are common. Again, in areas of deep incision, there are commonly more terrace levels than the regionally-common set. In places, workers recognize even higher $Q_I$ surfaces that are usually developed on the Paleozoic bedrock, significantly higher than the $Q_{II}$ terraces (e.g. Chediya, 1986), and are too poorly developed to address here.

Studies of pollen preserved in terrace gravels and correlative basin deposits show that the plant assemblages of the northern Kyrgyz Tien Shan during times of gravel aggradation were dominated by grasses with minor components of coniferous and small-leafed trees, suggestive of cold, dry conditions (Grigina and Fortuna, 1981). In records from basins with relatively continuous deposition, the intervening periods have pollen assemblages with greater fractions of tree pollen and more broad-leafed trees, which are interpreted to represent warmer, wetter interglacial climates similar to modern conditions (Grigina and Fortuna, 1981). The palynologic data thus support field relationships that suggest the terrace gravel aggraded contemporaneously with major late Pleistocene glacial advances.

Soviet era age control for the younger Quaternary terrace chronology was largely based on a limited number of numerical ages. The $Q_{IV}$ level is dated as Holocene with radiocarbon ages of 7.7 and 1.1 cal ka BP on the lower shoreline near the mouth of the Jergalan River (Fig. 2; Aleshinskaya et al., 1971; Trofimov, 1990; all reported radiocarbon ages are calibrated [Bronk Ramsey, 2009; Reimer et al., 2013], unless otherwise specified). Issyk-Kul lake sediments correlated as $Q_{III}^2$ near the Tyoup River, yielded a radiocarbon age of 31.3–29.4 cal ka BP (Fig. 2; Aleshinskaya et al., 1971). Thermoluminescence ages on older eastern Issyk-Kul basin sediments correlated with the river terraces suggest ages of 590–440 ka for $Q_I$, 320–280 ka for $Q_{II}^1$, and 230–220 ka for $Q_{II}^2$ (Trofimov, 1990).

Thompson et al. (2002) collected a suite of charcoal samples for radiocarbon dating from $Q_{III}^2$ and younger terraces in five basins west of Issyk-Kul, primarily from fine-grained sediment overlying terrace gravel. The ages of abandonment of $Q_{III}^2$ and $Q_{III}^3$ terrace levels are indistinguishable and consistent between basins in the range of 15.5–13.5 cal ka BP. Two radiocarbon ages within $Q_{III}^2$ fill along the Kajerty River in the Naryn basin southwest of Issyk-Kul (Fig. 1) are stratigraphically consistent at 47.9 ± 2.6 and 43.2 ± 3.3 ka BP, approximately in the middle of a thick $Q_{III}^2$ gravel fill deposit (Thompson, 2001). Infrared-stimulated luminescence dating of fine sediment capping terraces mapped as $Q_{II}^2$ in the Chu, Kochkor, and Naryn basins yielded overlapping ages, and assuming synchroneity, the best estimate of $Q_{II}^2$ terrace abandonment is 141 ± 17 ka (Thompson et al., 2002).

Selander et al. (2012) dated terraces along the Toru-Aygir River on the northern shore of Issyk-Kul using in-situ cosmogenic $^{10}Be$ dating of quartz pebbles collected in depth profiles. The model age for a terrace mapped as $Q_{III}^2$ is 85.6 ± 7.6 ka. Higher terraces correlated as $Q_{II}^1$ and $Q_{II}^2$ yielded ages of 139.9 ± 6.5 ka and 126.4 ± 10.8 ka, respectively.

### *1.3. Previous work on Issyk-Kul lake history*

Subaerial young lakebeds around Issyk-Kul coupled with the distinctive sub-lacustrine channels and terraces revealed in its bathymetry suggest that the lake level has fluctuated dramatically during the late Quaternary (Trofimov, 1978; De Batist et al., 2002). The history of Issyk-Kul is recorded in sediments from the deep basin as well as lake sediments exposed up to ~50 m above the modern lake level (Trofimov, 1990). A radiocarbon age estimate from a late Quaternary highstand at ~50 m higher than the modern lake is 31.3–29.4 cal ka BP and is correlated to the $Q_{III}^2$ river terraces (Aleshinskaya et al., 1971). Infrared-stimulated luminescence (IRSL) dating of feldspar grains associated with seismites in correlative lake sediment yielded age estimates of 26 to 10.5 ka (Bowman et al., 2004a).

Ricketts et al. (2001) obtained two ~ 4 m deep sediment cores from modern Issyk-Kul, and developed a radiocarbon chronology for the latest Pleistocene to recent by dating ostracodes. Their interpretations of geochemical variation through the sediment suggest that a previously smaller Issyk-Kul received a relatively large influx of meltwater in the early Holocene. They infer closure of the basin and a drop in lake level for a period 7 to 5 ka, followed by conditions more analogous to the present.

Early historical accounts of outflow suggest Issyk-Kul was at the sill level (~15 m above current, 1622 m amsl) during the period 1755–1858 CE (Ricketts et al., 2001). However, there is archeological evidence of human occupation of the lake floor to levels at least 6 m below the modern level, dated to the 13th to 15th centuries (Romanovsky, 2002). Previous radiocarbon ages on sediment at or below the young shoreline suggest that the lake was near the sill level during the period 400–1400 CE (Aleshinskaya et al., 1971; Ricketts et al., 2001; Romanovsky, 2002).

## 2. Methods

### *2.1. Terrace profiling*

We have documented the geometry of river terraces using the datum of the top surface of the terrace gravel, as this represents the position of the former floodplain prior to incision. In locations where the surficial sediment of a terrace tread is cover sediment rather than terrace gravel, we measured the elevation of the gravel/cover contact. We project the terrace gravel elevation data to smoothly curved valley-parallel lines in cases where the valleys are not linear. We profiled terrace surfaces with three techniques (Burgette, 2008): Quaternary geologic mapping (precision of 5–10 m), total station (precision 2–3 cm), and handheld mapping-grade differential GPS (precision ~ 0.5 m).

### *2.2. Radiocarbon dating*

We collected mollusk shells, charcoal and plant material from lake deposits and fine grained sediment overlying and underlying fluvial terrace gravels. Following manual cleaning, charcoal and wood samples were pretreated with acid-alkali-acid, and shell samples were pretreated with acid-only. Radiocarbon ages were measured by accelerator mass spectrometry (AMS), and results from three laboratories are all consistent with stratigraphic relationships where available (Table 1). All ages are calibrated with the IntCal13 dataset (Reimer et al., 2013) implemented in OxCal 4.2 (Bronk Ramsey, 2009), and ages discussed in the text are medians from the calibrated probability distributions in years before 1950 CE, unless otherwise specified. See Table 1 for full details of radiocarbon results.

### *2.3. Terrestrial cosmogenic nuclide (TCN) dating*

To constrain the ages of older terraces preserved in the southern Issyk-Kul area that are beyond the limit of radiocarbon dating (~45 ka), we collected samples of sediment to measure inventories of cosmogenic $^{10}Be$ in quartz. We collected most samples from terrace gravels in vertical profiles to assess the inherited proportion of $^{10}Be$ and verify post-depositional stability of the gravel deposits (Anderson et al., 1996; Phillips et al., 1998). We analyzed the 0.25–0.50 mm size fraction of the matrix of the terrace gravels, and analyzed ~15–30 g samples which contain thousands of individual grains, that well resolve the mean concentration of $^{10}Be$ for a given depth interval (Phillips et al., 1998). We selected sample sites based on the presence of an undisturbed gravel/cover contact, and minimal cover sediment thickness to ensure the surface TCN inventory had not been altered by erosion of the gravel deposit. We collected samples over ~6 cm depth ranges at intervals of 20–80 cm starting at the uppermost level of fluvial gravel, to a total depth of ≥200 cm.

The samples were processed in the geochronology laboratory at the University of Cincinnati. Quartz was chemically separated and leached following Kohl and Nishiizumi (1992). Following dissolution and addition of $^9Be$ carrier, Be was extracted using ion exchange chromatography. AMS measurements of $^{10}Be/^9Be$ ratios were made at the PRIME Laboratory, Purdue University.

**Table 1**
Radiocarbon ages for samples collected from Issyk-Kul lake and river terraces.

| Site | Sample name | Lab code[a] | Longitude (°E) | Latitude (°N) | Map code | Material | Height[b] (m) | $\delta^{13}C$[c] (‰) | Radiocarbon age[d,e] (yr) | Age range[f] (cal yr. B.P.; 95.4%) | Median age[f] (cal yr. B.P) |
|---|---|---|---|---|---|---|---|---|---|---|---|
| **Lake, Holocene shoreline** | | | | | | | | | | | |
| Tong bay | RBTG0805-1 | AA58092 | 76.9325 | 42.1551 | 1 | charcoal | −1.5 | −25.3 | 209 ± 30 | 305–0 | 178 |
| Tong bay | RBTG0805-5 | AA57667 | 76.9327 | 42.1576 | 2 | charcoal | −4.7 | −26.2 | 325 ± 30 | 471–306 | 388 |
| **Lake, late Pleistocene shoreline** | | | | | | | | | | | |
| Pristan | RWPRI-1 | CAMS111638 | 77.0147 | 42.1666 | 3 | shell | −1.2 | −4.3 | 20,650 ± 70 | 25,190–24,536 | 24,880 |
| Pristan | RWPRI-4 | CAMS111639 | 77.0127 | 42.1674 | 3 | root | −7.04 | −25 | 23,070 ± 1650 | 31,585–24,105 | 27,607 |
| Pristan | RBPRI-5 | AA57668 | 77.0118 | 42.1685 | 3 | shell | −12.58 | −9.1 | 33,680 ± 540 | 39,328–36,515 | 37,995 |
| Pristan | RWPRI-7 | CAMS111640 | 77.0123 | 42.1699 | 3 | shell | −15.46 | −3.8 | 37,560 ± 540 | 42,740–41,157 | 41,954 |
| Kok-Moynok | RWKM082704-S | CAMS111636 | 75.8702 | 42.4861 | 4 | shell | −10 | 0.5 | 22,710 ± 100 | 27,355–26,675 | 27, 077 |
| Ak-Terek | RB70305.1 | CAMS122060 | 76.7301 | 42.2568 | 5 | shell | −5.6 | 0 | 37,710 ± 470 | 42,718–41,391 | 42,056 |
| Ak-Terek | RB70305.2 | CAMS122061 | 76.7751 | 42.2388 | 6 | shell | −5.9 | 0 | 34,320 ± 310 | 39,637–38,251 | 38,845 |
| Ak-Terek | RB70305.3 | CAMS122062 | 76.7751 | 42.2388 | 6 | shell | −13.9 | 0 | 38,880 ± 530 | 43,714–42,080 | 42,818 |
| **$Q_{III}^{2}$ river terraces** | | | | | | | | | | | |
| Ak-Terek | RBATO912-2 | AA57659 | 76.6935 | 42.2093 | 7 | charcoal | 2.5 | −23.0 | 30,960 ± 420 | 35,788–34,122 | 34,913 |
| Ak-Terek | RBAT91604-1 | UCI35456 | 76.6935 | 42.2093 | 7 | charcoal | 2.5 | | 33,030 ± 360 | 38,300–36,299 | 37,212 |
| Ak-Terek | RBAT0824-V | AA57664 | 76.7102 | 42.2423 | 8 | oxidized wood | −5 | −8.8 | 40,500 ± 2800 | 49,973–41,685 | 44,948 |
| Ak-Terek | RBAT091404-1 | CAMS111637 | 76.6936 | 42.2130 | 9 | charcoal | −10.7 | −25 | >43,200** | | |
| Tong | RBTG091604 | CAMS111634 | 76.9064 | 42.1622 | 10 | charcoal | 1.8 | −24.0 | 1955 ± 40 | 1990–1824 | 1906 |
| Tong | RBTG092804 | CAMS111635 | 76.9203 | 42.1658 | 11 | charcoal | −16 | −25 | 39,850 ± 1430 | 46,920–41,725 | 43,882 |
| Tamga | RBTAM-1 | AA57665 | 77.5265 | 42.1491 | 12 | shell | 0.2 | −4.3 | 33,540 ± 550 | 39,143–36,379 | 37,820 |
| Tamga | RBTAM-2 | AA57666 | 77.5265 | 42.1491 | 12 | shell | 2.5 | −2.9 | 7178 ± 41 | 8153–7932 | 7990 |
| Tamga | RBTAM-3 | UCI35457 | 77.5265 | 42.1491 | 12 | charcoal | 3.9 | | 2950 ± 15 | 3171–3061 | 3113 |
| **$Q_{III}^{1}$ river terrace** | | | | | | | | | | | |
| Ak-Terek | RBAT0906-1 | AA57662 | 76.6809 | 42.2046 | 13 | shell | 0.2 | −8.2 | 37,640 ± 930 | 43,562–40,401 | 42,011 |
| Ak-Terek | RBAT0906-2 | AA57663 | 76.6809 | 42.2046 | 13 | shell | 0.2 | −7.0 | 39,300 ± 1100 | 45,346–41,775 | 43,324 |

[a] Samples with "AA" prefix analyzed at NSF - Arizona Accelerator Mass Spectrometry Laboratory; "CAMS" prefix: Center for Accelerator Mass Spectrometry, Lawerence Livermore National Labs; "UCI" prefix: University of California, Irvine Accelerator Mass Spectrometry Laboratory.
[b] Height above top of gravel for river terraces, above top of local outcrop for lacustrine sediments.
[c] $\delta^{13}C$ values are the assumed values according to Stuiver and Polach (1977) when given without decimal places. Values measured for the material itself are given with a single decimal place. Fractionation effects are accounted for in the AMS measurement process for UCI samples.
[d] The quoted age is in radiocarbon years using the Libby half life of 5568 years and following the conventions of Stuiver and Polach (1977).
[e] CAMS# 111637 is reported as a 2-sigma limit as per Stuiver and Polach (1977).
[f] Calibrated using OxCal 4.2 (Bronk Ramsey, 2009), using the IntCal13 calibration curve (Reimer et al., 2013).

Concentrations of $^{10}Be$/g quartz are corrected for process blanks, with errors propagated following the procedure outlined by Balco et al. (2008). We determined model ages using the online CRONUScalc program (Marrero et al., 2016), using time-dependent rates from the Lifton et al. (2014b) nuclide-dependent scaling scheme and updated calibration data (Borchers et al., 2016). Production rates are modified for topographic shielding (negligible for all sites here) and the thickness of the sampled interval.

$^{10}Be$ concentrations and uncertainties at the upper gravel surface of each profile are estimated with linear regression applied to the full datasets of each depth profile (Burgette, 2008). As the measured concentration-depth profiles in the gravel are largely insensitive to the history of covering sediment (Gosse and Phillips, 2001), we estimate bracketing age scenarios using end-member cover histories. The limiting minimum age assumes no cover sediment was present over the history of the terrace surface (all of the present cover sediment was deposited very recently). The maximum age assumes the presently-observed cover sediment thickness has been present since abandonment of the terrace. We calculate the factor by which the cover sediment attenuates the production rate due to spallation using an attenuation length of 160 g $cm^{-2}$ (Gosse and Phillips, 2001), and estimates of cover sediment density. The maximum ages are calculated with the CRONUScalc program (Marrero et al., 2016), with the attenuated production rate controlled by modifying the topographic shielding parameter. These cases bracket the most likely scenario of the thickness of the capping sediment progressively accumulating through time.

## 3. Results

### 3.1. Issyk-Kul lake history

We focus on resolving ages for the two prominent shorelines above the modern lake level. The lower shoreline rings Issyk-Kul at an elevation of ~1622 m amsl, consistent with a lake surface at the elevation of the modern sill at the western end of Issyk-Kul. The higher shoreline is more discontinuously preserved as a break in slope at an elevation of 1650–1680 m amsl.

We radiocarbon dated the younger high stand (~1622 m amsl) in the bay at the mouth of the Tong River (Fig. 4a) using organic material from two horizons in a package of lacustrine sediment. The elevation of top of the deposit is ~1620 m amsl, and the sediment was likely deposited while the lake was at or rising to the 1622 m amsl sill level. The lower sample yielded an age of ~ 1500–1650 CE, and the sample from 3.2 m higher stratigraphically has an age range of 1640–1960 CE (Table 1). These ages are consistent with Issyk-Kul rising to its overflow level following the archeologically-dated lowstand. The lake likely remained high through the earliest written accounts of the lake level (Ricketts et al., 2001), as suggested by the continuous section of bedded lake sediment we sampled.

The higher shoreline is best expressed along the western to central southern Issyk-Kul basin as a prominent topographic break at the base of a cliff that truncates badlands topography developed on Neogene clastic sediments (Figs. 2 and 4). Areas where the break in slope is at elevations >1660 m amsl generally correspond with thick colluvial and slope wash wedges shed from the adjacent cliffs.

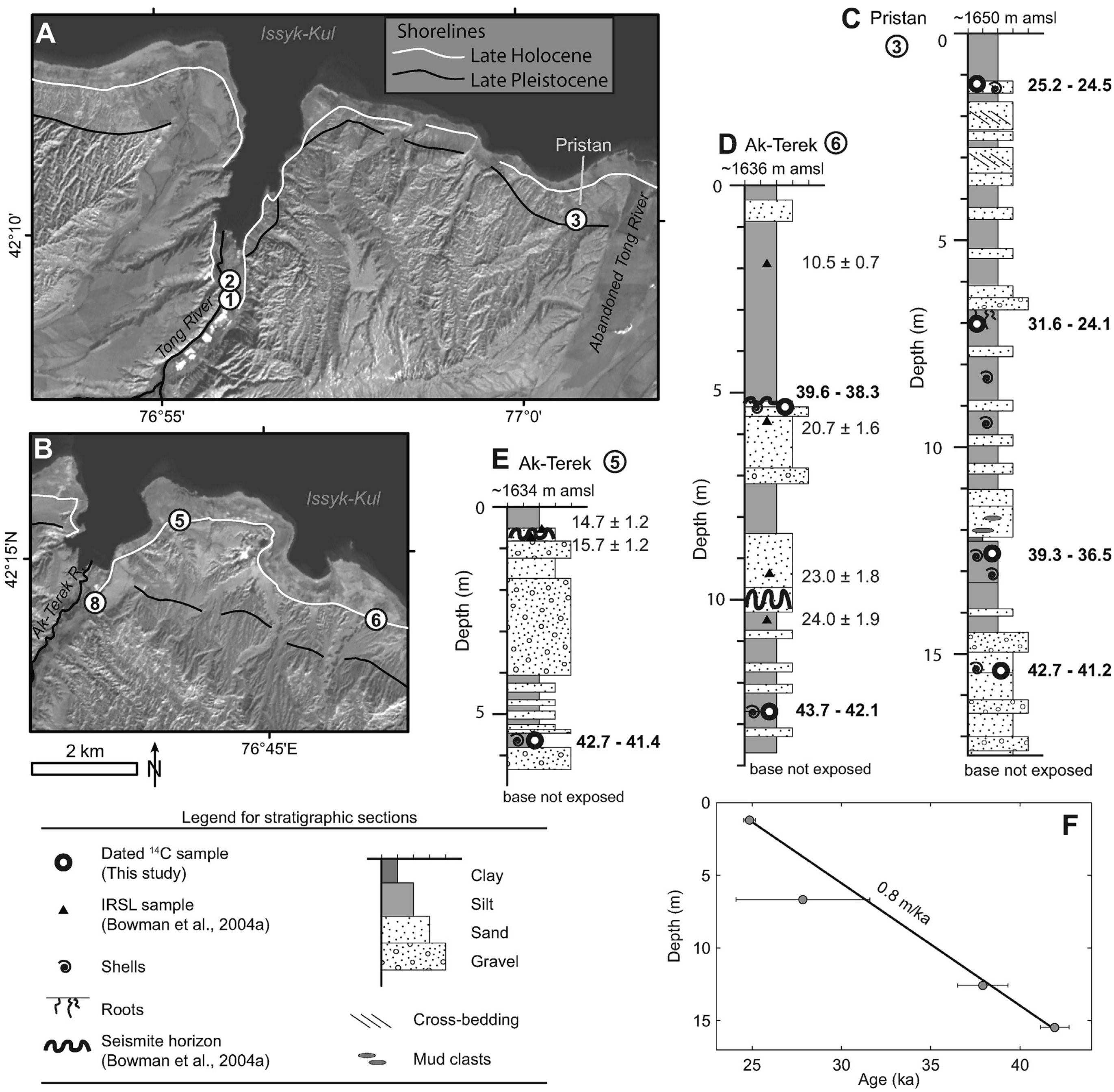


**Fig. 4.** Location, stratigraphy, and radiocarbon dating of late Quaternary shorelines. (a) and (b) Maps of sample locations in the Tong and Ak-Terek areas, respectively (ASTER image, band 3); see Fig. 2 for locations. White and black lines show the Holocene and higher late Pleistocene remnant shorelines, respectively. Numbers of sample locations correspond to Table 1. (c), (d), and (e) Stratigraphic sections showing positions of samples analyzed in this study and relationship to previous IRSL chronology in Ak-Terek area. Sample ages given in ka. (f) Age-elevation history of lake sediment deposition at Pristan site.

Canyons expose continuous sections of lacustrine sediment between ~1620 and 1660 m amsl. The shoreline is absent where cross-cut by younger river terraces and active alluvial fans. In the eastern end of the Issyk-Kul basin, the shoreline is expressed only as a break in slope cut into the limbs of low relief active folds that have uplifted the Neogene section. We investigated and dated Issyk-Kul lacustrine sections associated with the higher shoreline in three locations along the southern shore and in the northwestern arm of Issyk-Kul: Pristan, Ak-Terek, and Kok-Moynok (Fig. 2).

The Pristan site lies near the mouth of the abandoned course of the Tong River (Fig. 4a). We sampled >15 m of near-shore lacustrine stratigraphy exposed in an irrigation-related gully (Fig. 4c). Laterally continuous beds are traceable over the ~150 m long gully. Roots associated with a surface at a depth of 6.7 m are the only evidence for a significant unconformity breaking the depositional sequence. The section consists of well-sorted, interbedded layers of silt and sand, with some pebble gravel beds at depths >14.5 m and immediately above the horizon with roots (Fig. 4c). Radiocarbon dating of four root and shell samples yield ages consistent with an average rate of deposition of 0.8 m/ka over the period 42–25 cal ka BP (Fig. 4f, Table 1). As the top of dated section is a few meters below the erosional shoreline angle of the highstand, the upper age of ~25 cal ka BP represents a minimum for the end of the late Pleistocene high lake level. While we lack direct evidence for or against uplift of these lake deposits from the elevation where they were deposited, the average uplift rate must have been lower than the rate of transgression over the >18 ka period of high lake level.

We dated lake sediment between the two shorelines east of the mouth of the Ak-Terek River that were previously dated using a single aliquot IRSL method (Bowman et al., 2004a, Fig. 4b). We sampled mollusk shells from lacustrine sediment exposed in the cliff above the historical (~1622 m amsl) shoreline. Thus, in comparison to the Pristan section, these samples come from lower elevation and farther from the local shoreline of the eventual highstand. We radiocarbon dated one sample from the lower part of "station 11" of Bowman et al. (2004a). This sample yielded an age of 42.1 cal ka BP, and lies only 4.6 m below layers that yielded IRSL ages of 15.7 and 14.7 ka (Fig. 4e). Our other samples come from an outcrop ~5.5 km east of the Ak-Terek River mouth ("station 15" of Bowman et al. (2004a); Fig. 4b). Ages of our radiocarbon samples in this section are 42.8 cal ka BP and 38.8 cal ka BP, below and interbedded with IRSL samples in the range of 24.0 to 10.5 ka (Fig. 4d). Additionally, we radiocarbon dated oxidized wood preserved in lacustrine fill below the $Q_{III}^{3}$ and $Q_{III}^{2}$ terraces near the mouth of the Ak-Terek River (Fig. 4b). This sample yielded an age of 44.9 cal ka BP, consistent with the oldest ages of the shoreline deposits, although near the limit of the radiocarbon technique.

As the Ak-Terek area dated sections are both low in the total lacustrine section relative to Pristan, the measured ages are consistent with the lowest exposed lake deposits having been deposited >43 cal ka BP. However, there is a clear mismatch between the ages obtained via the IRSL and radiocarbon methods from the same sediments, with the IRSL ages being systematically younger by ~19 ka. Calibration of the radiocarbon ages cannot explain the discrepancy, as the calibration curve is well constrained for the age range implied by the IRSL dating (Reimer et al., 2013). While all of the radiocarbon samples except for the in situ root of sample RW-PRI-4 at Pristan are from mollusk shells, the excellent age-elevation relationships we obtain from the radiocarbon ages from single outcrops and correlation between sites suggest that significant recycling is unlikely to be responsible for the observed discrepancies. The ~840 yr residence time observed in modern lake carbonate shells (Ricketts et al., 2001), suggests reservoir effects are also unlikely to explain the inconsistency. The IRSL measurements were not corrected for possible fading and there were likely temporal variations in dose rate due to moisture content changes in the lake sediment and erosion of shielding sediment. Given these uncertainties, and the more consistent radiocarbon age-elevation relationships, we prefer the age control from the radiocarbon dating to define the lake history.

The third location where we obtained estimates of lake sediment age is from the Kok-Moynok basin, west of modern Issyk-Kul (Fig. 2). The total thickness of currently subaerial lacustrine material in Kok-Moynok is thicker than observed elsewhere in the Issyk-Kul basin, reaching ~100 m, where the river canyon exposes levels below the modern lake. At the time of the deposition of the Kok-Moynok lakebeds, Issyk-Kul extended farther west, with the Chu River emptying into the lake west of the modern sill (Fig. 2). The similar elevation of the uppermost lake sediments preserved in the Kok-Moynok basin and the upper shoreline in the broader Issyk-Kul basin suggests that these sediments record the same highstand (Burgette, 2008). This inference is corroborated by a radiocarbon age of 27.1 cal ka BP from a sample of shell we collected at a stratigraphic level 70% above the base of the deposit. This age is correlative with the middle to upper portion of the Pristan section (Table 1).

### 3.2. Fluvial terrace development in southern Issyk-Kul

Flights of well-developed terraces flank most of the rivers that drain out of the Terskey Range into the southern margin of Issyk-Kul. Given the diversity of faults and folds that have actively deformed the southern margin of Issyk-Kul during the Quaternary, different rivers experience varying rates of rock uplift along their lengths, leading to varying patterns of incision and aggradation. We have studied terraces associated with eight southern Issyk-Kul rivers (Burgette, 2008). Here we focus on the three best examples: the Ak-Terek River in the west, and the Barskaun and Jety-Oguz Rivers in the eastern basin (Fig. 2).

#### 3.2.1. Ak-Terek River

The Ak-Terek River maintains the only water gap in a 40 km long granitic bedrock ridge, which is uplifted by a south-vergent reverse fault against the regional northward slope down from the Terskey Range (Fig. 2). Downstream of the gorge through the basement block, a set of terraces is well preserved, although deformed by two south-vergent faults and related fold pairs (Fig. 5a). In the northern Ak-Terek area an extensive $Q_{II}$ terrace caps the local topography as the terrace gravel is more resistant to erosion than the siltstone and interbedded sandstones of the upper Neogene section (Fig. 5a). Where terrace sediments are well exposed they are composed of cobble gravel that is generally <5 m thick.

$Q_{III}$ terraces are inset into the broad $Q_{II}$ surface, along the modern Ak-Terek River canyon (Fig. 5a). Two prominent terraces, $Q_{III}^{1}$ and $Q_{III}^{0.5}$, are preserved in the northern portion of the area, and likely merge into a single aggradational surface in the synclinal Bar-Bulak valley, labeled $Q_{III}^{0.5/1}$. The paired $Q_{III}^{0.5/1}$ terrace appears to bury the more steeply dipping $Q_{II}$ surface at the southern edge of the valley (Fig. 5a). The base of this $Q_{III}^{0.5/1}$ fill deposit is not well exposed, but at least 20–30 m of cobble gravel accumulated in the active syncline.

The youngest prominent terraces are subtly distinct paired $Q_{III}^{2}$ and $Q_{III}^{3}$ surfaces that diverge downstream from a common surface in the Bar-Bulak synclinal valley (Fig. 5a). Interbedded fluvial and lacustrine sediment below the $Q_{III}^{2}$ surface extends below the level of the modern river and tributary gullies along most of the river. Where visible, the basal unconformity of the $Q_{III}^{2}$ fill is irregular, burying underlying topography. The $Q_{III}^{3}$ terrace is cut into the $Q_{III}^{2}$ fill on the east side of the river, and has a strath morphology on the west side of the river where ~2 m of gravel overlie Neogene rock. At the mouth of the river, the uppermost $Q_{III}^{2}$ terrace gravel is sandwiched between two distinct packages of lacustrine sediment, which we interpret to have been deposited during the late Pleistocene high stand of Issyk-Kul. The inset $Q_{III}^{3}$ terrace cuts through the lacustrine sediment and extends north to where it is truncated by the ~1620 m late Holocene shoreline (Fig. 5a).

*3.2.1.1. Ak-Terek profiles.* Profiles of the Ak-Terek river terraces constructed from total station surveys and topographic and bathymetric maps show the results of terrace formation during progressive tectonic deformation and lake level fluctuations (Fig. 5c and d). The linear portion of the modern river profile is 1.2°, and becomes concave over the northern 4 km of the profile, near Lake Issyk-Kul (Fig. 5c and d). Below the modern lake surface, the bathymetry shows an alluvial fan deposited at the mouth of the Ak-Terek River, bisected by a canyon. Extrapolation of the younger $Q_{III}$ terrace profiles to the top of the alluvial fan suggests that the $Q_{III}^{2}$ and/or $Q_{III}^{3}$ Ak-Terek River were the source of the fan sediment. The northern edge of the alluvial fan is convex, steepening toward the central lake floor. The canyon incised into the fan extends to ~100 m below the modern lake level, and it the offshore portion of this canyon projects to the profile of the modern river upstream of the

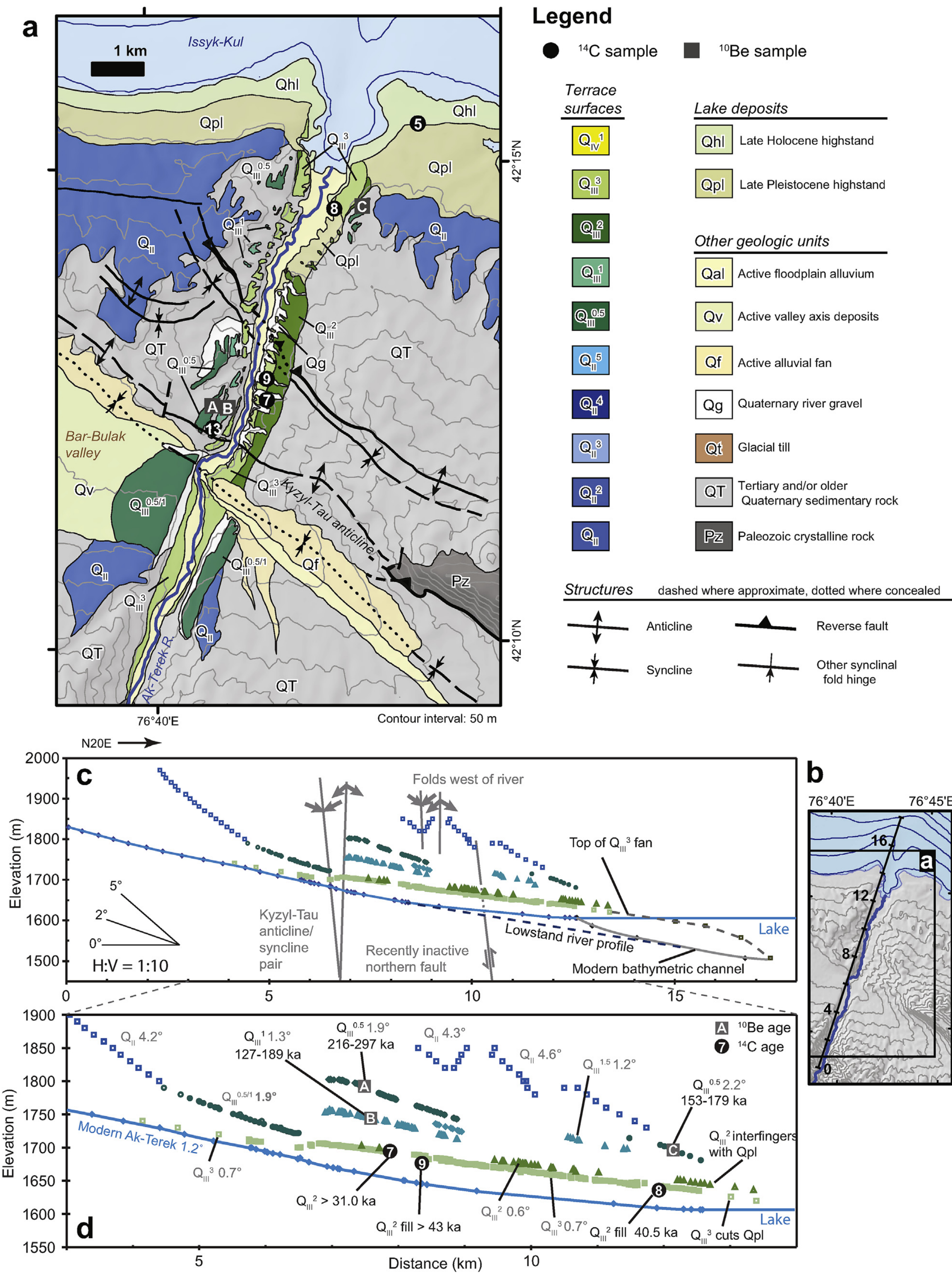


**Fig. 5.** (a) Quaternary geology and geomorphology of the Ak-Terek River area. (b) Map showing broader area and profile line, with distances indicated in km. (c) Long profile of river terraces along the Ak-Terek River and positions of Quaternary structures. Filled symbols show points surveyed with a total station, and open symbols were digitized from 10 m contour topographic maps. (d) More detailed view of central profile, with slopes of terrace remants, dated sample locations, and ages indicated.

flat reach that is graded to the modern lake surface (Fig. 5c). The submerged channel suggests that the local concavity of the northernmost modern Ak-Terek River is due to an ongoing adjustment to the latest Holocene highstand via deposition in the lowest reach. Terrace remnants are quite planar except for offsets across localized structures, which suggests the nonlinear modern river profile is not representative of the conditions when the terraces were abandoned (Fig. 5d). The slope of the $Q_{III}^{3}$ terrace is 0.7° on both sides of the Kyzyl-Tau anticline, lower angle than the modern incised river, but steeper than 0.6° $Q_{III}^{2}$ fill surface.

All of the $Q_{III}$ and $Q_{II}$ terraces are progressively deformed across the Kyzyl-Tau anticline-syncline pair, and the pre- $Q_{III}^{2}$ terraces are also offset by the faulted fold to the north. Although it is difficult to match the higher surfaces across the fault to the north, there has been considerable offset across this structure. However, the $Q_{III}^{3}$ surface, which is clearly warped across the southern Kyzyl-Tau fold pair, exhibits little to no deformation at the northern fault. The $Q_{II}$ terraces are offset by an additional fold pair that dies out west of the $Q_{III}$ terrace remnants. Terraces slope northward at progressively steeper angles with age across the entire profile length, and correlative terraces have similar angles away from the active structures. This long-wavelength progressive northward tilting reflects the uplift of the Terskey Range (Burgette, 2008).

*3.2.1.2. Ak-Terek chronology.* The geologic and geomorphic relationships between the dated lake sections and the younger terraces strongly constrain the ages of $Q_{III}^{2}$ and $Q_{III}^{3}$. The gravel of the $Q_{III}^{2}$ terrace is clearly older than the youngest late Pleistocene lakebeds. However, the upper part of the $Q_{III}^{2}$ terrace gravel also overlies older lakebeds at the mouth of the river, as well as upriver. We have two direct radiocarbon ages for the lacustrine and alluvial fill below $Q_{III}^{2}$ showing they are ~43 cal ka BP or older (Fig. 5d; Table 1). Ages for charcoal from a burn horizon in cover sediment on the $Q_{III}^{2}$ terrace yield limiting young ages of 34.9 and 37.2 cal ka BP, indicating the top of the $Q_{III}^{2}$ fill must have been at least locally abandoned by that time. Abandonment of the inset $Q_{III}^{3}$ level is broadly bracketed by the youngest sediment of the late Pleistocene high stand (<25 cal ka BP), and the late Holocene high stand at the modern sill elevation.

To define the ages of the older $Q_{III}^{1}$ and $Q_{III}^{0.5}$ terraces we collected $^{10}$Be profile samples from pits 0.5 km north of the Kyzyl-Tau anticlinal hinge (Fig. 5). The sampled $Q_{III}^{0.5}$ terrace forms the local hilltop, and the $Q_{III}^{1}$ sample site is at the distal fringe of a wedge of slopewash and colluvial sediment shed off of the riser up to $Q_{III}^{0.5}$. $^{10}$Be depth profiles show well-constrained exponential decreases in the concentration of $^{10}$Be with depth, consistent with the relative ages of the terraces (Fig. 6a and Table 2). Since the samples came from the interiors of terrace remnants, there is little possibility that the coarse gravel has been eroded since the abandonment of either surface. The low $^{10}$Be concentrations at the maximum sampled depths suggest a minimal inherited contribution to the observed inventory, implying relatively rapid erosion and transport rates in the upstream portion of the catchment (Fig. 6a).

The greatest uncertainty associated with converting the measured $^{10}$Be concentrations to model ages relates to the history of the fine-grained cover material overlying the terrace gravel. The lack of gullies developed on the smooth surface of the cover wedges suggests that there has not been significant degradation of the capping wedges. By assuming a time-averaged zero thickness for the shielding material, we calculate robust minimum $^{10}$Be depth profile ages of 216 and 127 ka for $Q_{III}^{0.5}$ and $Q_{III}^{1}$, respectively (Table 2). If the current thicknesses of the covering sediment formed instantly upon terrace abandonment, the ages would be 279 and 189 ka, respectively, using a cover sediment density of 1.5 g/cm$^3$ (Table 2). A scenario where the fine-grained cap grew

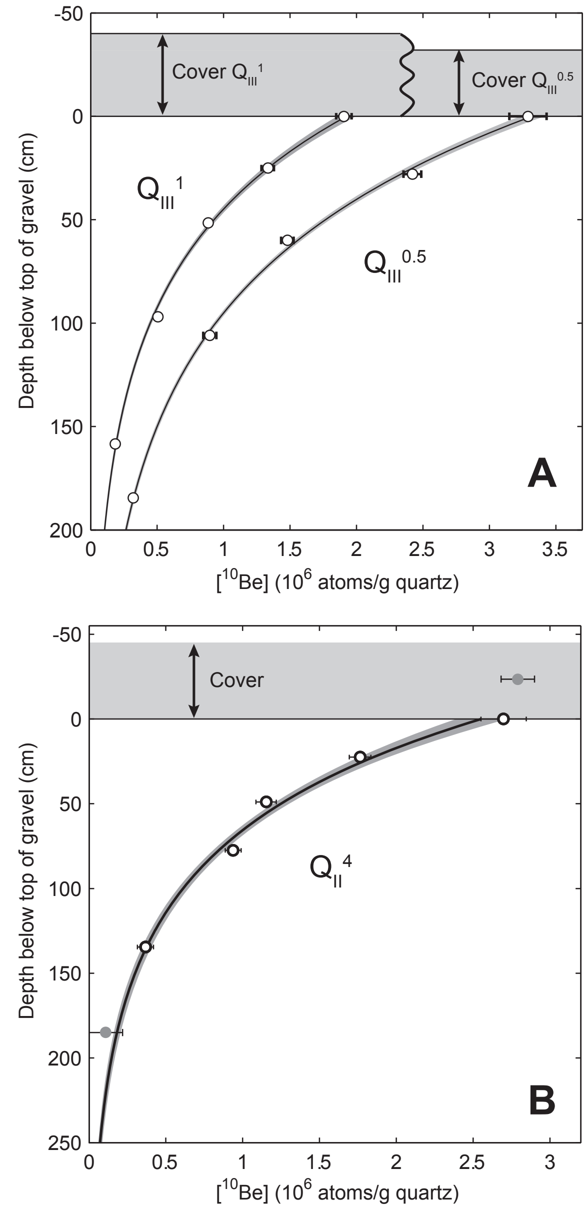


**Fig. 6.** $^{10}$Be depth profiles for terraces. (a) Ak-Terek. (b) Jety Oguz; Black curves with gray background are model ± 1 standard error used in age estimation. Gray samples excluded from model age calculation as discussed in text. Shaded gray layers above the profiles show fine grained cover sediment at the sample locations.

monotonically through time would yield an age bracketed by these two estimates.

A $^{10}$Be age of 196–140 ka was obtained for granitic cobbles on the surface of the $Q_{III}^{0.5}$ terrace near the mouth of the Ak-Terek River (Fig. 5, Table 2). This age range reflects clast degradation rates from 0 to 0.001 mm/yr, and 1σ uncertainties from the CRONUS calculator (Marrero et al., 2016) propagated from analytical and calibration uncertainties. As this age is at least 20 ka younger than the robust minimum of the profile age for this terrace upstream, it appears that the surface cobbles were unlikely to have been exposed at the surface over the entire terrace history. A greater clast surface denudation rate is unlikely to explain the discrepancy, as the bracketing maximum erosion rate we use implies the sampled cobbles lost nearly 18 cm of material. Such erosion seems unlikely given the rounded, equant appearance of the clasts and their

**Table 2**
Cosmogenic nuclide dating sample information.

| Sample | Latitude (°N) | Longitude (°E) | Elevation (m amsl) | Map code | Depth (cm) Min | Max | Mean | Thickness (cm) | Topographic shielding[a] | $^{10}$Be Concentration[b] ($10^6$ atoms/g quartz) | Standard | Minimum age[c] (ka) | Maximum age[c] (ka) |
|---|---|---|---|---|---|---|---|---|---|---|---|---|---|
| **Ak-Terek $Q_{III}^1$ profile** | | | | B | | | | | | | | | |
| RBATQ32-1 | 42.2081 | 76.68435 | 1743 | | 37 | 43 | 40 | 6 | 0.9992 | 1.90 ± 0.06 | 07KNSTD | 127 ± 11 | 189 ± 15 |
| RBATQ32-2 | 42.2081 | 76.68435 | 1743 | | 62 | 68 | 65 | 6 | 0.9992 | 1.33 ± 0.05 | 07KNSTD | | |
| RBATQ32-3 | 42.2081 | 76.68435 | 1743 | | 87 | 96 | 91.5 | 9 | 0.9992 | 0.88 ± 0.02 | 07KNSTD | | |
| RBATQ32-4 | 42.2081 | 76.68435 | 1743 | | 133 | 141 | 137 | 8 | 0.9992 | 0.51 ± 0.02 | 07KNSTD | | |
| RBATQ32-5 | 42.2081 | 76.68435 | 1743 | | 194 | 203 | 198.5 | 9 | 0.9992 | 0.18 ± 0.01 | 07KNSTD | | |
| **Ak-Terek $Q_{III}^{0.5}$ profile** | | | | A | | | | | | | | | |
| RBATQ31-1 | 42.2085 | 76.68078 | 1792 | | 29 | 35 | 32 | 6 | 0.9999 | 3.29 ± 0.14 | 07KNSTD | 216 ± 19 | 297 ± 25 |
| RBATQ31-2 | 42.2085 | 76.68078 | 1792 | | 58 | 62 | 60 | 4 | 0.9999 | 2.42 ± 0.07 | 07KNSTD | | |
| RBATQ31-3 | 42.2085 | 76.68078 | 1792 | | 89 | 95 | 92 | 6 | 0.9999 | 1.48 ± 0.05 | 07KNSTD | | |
| RBATQ31-4 | 42.2085 | 76.68078 | 1792 | | 134 | 142 | 138 | 8 | 0.9999 | 0.90 ± 0.05 | 07KNSTD | | |
| RBATQ31-5 | 42.2085 | 76.68078 | 1792 | | 213 | 220 | 216.5 | 7 | 0.9999 | 0.32 ± 0.01 | 07KNSTD | | |
| **Ak-Terek $Q_{III}^{0.5}$ surface cobbles** | | | | C | | | | | | | | | |
| SCT/270801/1 | 42.2427 | 76.71667 | 1690 | | | | | 1 | 0.9999 | 2.64 ± 0.06 | LLNL3000 | 153 ± 13 | 179 ± 17 |
| **Jety Oguz $Q_{II}^4$ profile** | | | | D | | | | | | | | | |
| RBJO1 | 42.4176 | 78.2337 | 1960 | | 19 | 24 | 21.5 | 5 | 0.9997 | 2.79 ± 0.11 | KNSTD | 129 ± 14 | 219 ± 25 |
| RBJO2 | 42.4176 | 78.2337 | 1960 | | 42 | 48 | 45 | 6 | 0.9997 | 2.70 ± 0.15 | KNSTD | | |
| RBJO3 | 42.4176 | 78.2337 | 1960 | | 64 | 71 | 67.5 | 7 | 0.9997 | 1.76 ± 0.07 | KNSTD | | |
| RBJO4 | 42.4176 | 78.2337 | 1960 | | 91 | 97 | 94 | 6 | 0.9997 | 1.15 ± 0.07 | KNSTD | | |
| RBJO5 | 42.4176 | 78.2337 | 1960 | | 120 | 125 | 122.5 | 5 | 0.9997 | 0.94 ± 0.05 | KNSTD | | |
| RBJO6 | 42.4176 | 78.2337 | 1960 | | 175 | 184 | 179.5 | 9 | 0.9997 | 0.37 ± 0.05 | KNSTD | | |
| RBJO7 | 42.4176 | 78.2337 | 1960 | | 225 | 235 | 230 | 10 | 0.9997 | 0.11 ± 0.11 | KNSTD | | |
| **Jety Oguz modern river** | | | | E | | | | | | | | | |
| RBJOR | 42.41127 | 78.21751 | 1810 | | | | | | | 0.03 ± 0.03 | KNSTD | | |

Errors are 1 σ and reflect the analytical errors of samples and external uncertainty from age calibration.
Minimum ages assume no erosion for surface samples, and no sediment covering profile samples.
Maximum ages assume an erosion rate of 0.001 mm/yr for surface samples and present cover sediment thickness over history of terrace.
[a] Shielding calculated with CRONUS online calculator (Balco et al., 2008).
[b] Concentrations are corrected for process blanks, uncertainty is 1σ, propagated following Balco et al. (2008).
[c] Calculated with CRONUS online calculator (Marrero et al., 2016) using time-dependent production rates from the Lifton et al. (2014b) nuclide-specific scaling scheme.

similarity to deeper, pristine portions of the terrace gravel.

The terrace ages are consistent with relatively constant rates of river incision and deformation over the late Pleistocene when averaged over multiple cycles of terrace formation (Fig. 7). Abandonment of the $Q_{III}^3$ terrace is well defined to occur after the 25 cal ka BP age of the youngest late Pleistocene lake sediment that we dated, and we use a 12 cal ka BP minimum age based on incision of $Q_{III}^2$ and $Q_{III}^3$ terraces dated in the basins to the west (Thompson et al., 2002). The good fits of the linear models to either of the cover scenarios (minimum and maximum ages) for the $^{10}$Be chronology suggests that the $Q_{III}^{0.5}$ and $Q_{III}^1$ terraces did not have greatly different cover histories from one another (Fig. 7). The modern river clearly lies off of the long-term incision-age trajectory, and the 1.2° modern slope of this reach is much steeper than the 0.6° intercept of the slope-age relationship (Fig. 7), consistent with the modern river and dated late Quaternary terraces representing different stages in the terrace-forming cycle.

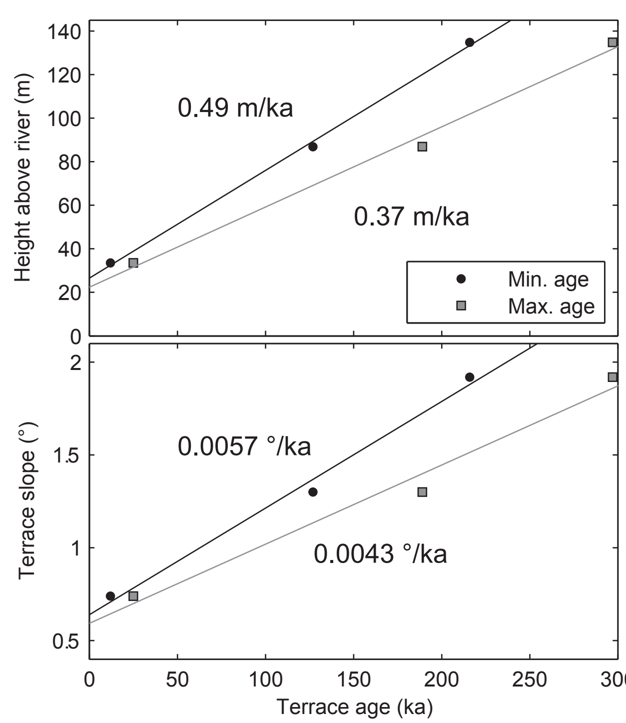


**Fig. 7.** Rates of incision of Ak-Terek River from the dated terrace sequence and rates of tilting for the two age scenarios. The linearity of the age evolution suggests that the shielding history of the two upper terraces dated with $^{10}$Be did not differ substantially.

### 3.2.2. *Barskaun River*

The Barskaun River is the largest river that drains into south-central Issyk-Kul, emerging north out of a deep glacial trough in the Terskey Range (Fig. 2). The Barskaun River has deposited an extensive $Q_{III}^2$ alluvial fan at its mouth that extends below the modern lake level (Figs. 2 and 8a). East of the Barskaun River, we recognize a partially dissected $Q_{II}$ surface where fine-grained slope wash and/or loess deposits mantle a surface cut across a thick earlier Quaternary boulder gravel deposit (Fig. 8a). A higher, more gently sloping $Q_{II}$ surface is beveled across the highest hilltop north of the contact with the Paleozoic basement on the west side of the Barskaun. $Q_{III}^1$ terraces are inset 150–200 m below and parallel to the $Q_{II}$ surface in the canyon. The $Q_{III}^1$ and $Q_{II}$ terraces appear to merge at the steeper rangefront. For both the $Q_{III}^1$ and $Q_{II}$ surfaces, there is little clast-supported gravel overlying the matrix-supported boulder gravel across which the surfaces are cut.

An extensive $Q_{III}^2$ terrace is inset well into the coarse sediment capped by the $Q_{II}$ and $Q_{III}^1$ surfaces, which forms the prominent fan surface at the mouth of the canyon (Fig. 8a). The Barskaun $Q_{III}^2$ terrace coalesces with an alluvial fan terrace at the mouth of the Tamga River to the west. Exposures below the $Q_{III}^2$ terrace show >100 m of gravel, with no exposure of underlying Neogene sedimentary rock. In contrast to the deposit underlying the $Q_{II}$ terrace, the $Q_{III}^2$ gravel is clast-supported, with rounded clasts that range from pebble to boulder size (up to 4 m in maximum dimension). The gravel deposit is generally massive with the exception of a mud-cemented layer that stands out in relief from the surrounding walls ~ 2–3 km upstream from the river mouth.

The fan shaped $Q_{III}^2$ surface is pristine with no significant sublevels. The northern edge of the terrace surface is truncated by a 2–20 m cliff down to the late Holocene shoreline. The only suggestion of a higher lake level preserved on the surface is a small remnant of sediment with a maximum elevation of ~1648 m amsl that forms a wedge thickening toward the lake near the eastern edge of the $Q_{III}^2$ alluvial fan (Fig. 8a).

*3.2.2.1. Barskaun profiles.* Barskaun River terrace profiles collected with GPS and from topographic maps are projected to a smoothly curved line that generalizes the modern Barskaun inner canyon and alluvial fan axis (Fig. 8b and c). The profiles collected from the west and east sides of the $Q_{III}^2$ surface show that this terrace is precisely paired across the modern canyon. The overall shape of the $Q_{III}^2$ terrace in profile is well approximated by a slope of 1.8°, with a possible convexity of ~0.10° over the 10 km surveyed reach (Fig. 8c). Bathymetric data from the top of the sub-lacustrine fan surface project to the subaerial portion of the $Q_{III}^2$ surface (Fig. 8c). The alluvial fan steepens below a depth of 50 m to a mean slope >3°. Surveyed points collected on the top of the resistant mud-cemented bed in the $Q_{III}^2$ gravel yielded a slope of 2.8°. This steeper internal stratigraphy suggests that constant-age horizons in the $Q_{III}^2$ gravel may not parallel the top of the terrace surface. This could result from the alluvial fan prograding northward rather than through parallel vertical growth over its entire modern extent, or that the progressive northward tilting extends north across the lake shoreline.

In contrast to the linear profile of the $Q_{III}^2$ terrace, the modern Barskaun River shows a more complex geometry that we infer is transient (Fig. 8c). In the upper reach of the profile, the modern lies only ~20 m below the top of the $Q_{III}^2$ gravel. The river steepens from a slope of ~2.0° in this southern reach to a maximum value of ~2.6° at a profile distance of 6.2 km. North of the steepest reach, the profile is abruptly concave, decreasing to a slope of 0.3° over a profile distance of 3 km (Fig. 8c). This reach of the river coincides with the transition from a straight to braided channel habit. The lake bathymetry reveals a canyon cut through the axis of the offshore fan at the mouth of the Barskaun River. This submerged canyon is incised to ≥100 m below the modern lake surface, and its profile projects to the steeper subaerial reach.

We interpret this complex profile of the modern river and offshore channel to have formed initially by incision of a canyon through the $Q_{III}^2$ alluvial fan following lake regression. The subsequent late Holocene highstand raised base level and caused deposition of a wedge of sediment in the downstream portion of the canyon. The sub-lacustrine steep face of this wedge represents foreset beds of a growing delta, potentially analogous to the growth of the lower part of the $Q_{III}^2$ fan, as shown by its basal bathymetry and the geometry of the indurated bed.

The older terraces that cap the topography along the rangefront dip much more steeply northward than the $Q_{III}^2$ terrace (Fig. 8c). The highest $Q_{II}$ surface dips 5.6° along the profile and ends to the south at a much steeper hillslope developed across the older Quaternary sediment. The profiled $Q_{III}^1$ terraces show a localized steepening near the rangefront, but do not match one another in detail across the canyon, likely in part due to the change in rangefront orientation across the Barskaun River (Fig. 8a and c). In spite of the complications of the terrace geometries, it is clear that terraces are progressively tilted with age along the rangefront.

*3.2.2.2. Barskaun chronology.* Over most of the broad $Q_{III}^2$ terrace, there is < 0.5 m of cover sediment overlying the terrace gravel. However, on the far western edge of the $Q_{III}^2$ alluvial fan, west of the Tamga River, a $Q_{III}^1$ terrace remnant sheds fine-grained colluvial and slopewash deposits onto $Q_{III}^2$ gravel (Fig. 8a). We collected three radiocarbon samples through this 4.95 m thick wedge near the riser to the $Q_{III}^1$ terrace where exposed in a young gully. The lowest radiocarbon age of 37.8 cal ka BP is on terrestrial gastropod shells from a 30 cm thick package of well-bedded sand and silt immediately overlying the $Q_{III}^2$ gravel (Table 1). Shells from an extremely shell-rich layer midway through the section (2.5 m above the gravel) yielded a radiocarbon age of 8.0 cal ka BP. The uppermost sample we dated is charcoal and comes from 1.4 m higher, ~1 m below the surface of the colluvial section, yielding an age of 3.1 cal ka BP.

The ages from the section overlying the $Q_{III}^2$ gravel at Tamga suggest that deposition on the terrace following abandonment spanned >30 ka, with half of the thickness accumulating in the past 8 ka, before the recent onset of gullying. The setting and stratigraphy of the dated section suggests that aggradation of the $Q_{III}^2$ surface had reached the upper surface, at least at this location on the Barskaun fan, prior to ~38 cal ka BP, during the middle to early part of the late Pleistocene lake highstand. The fact that evidence of this highstand is not preserved across the $Q_{III}^2$ alluvial fan (except perhaps the local outcrop at the northeastern Barskaun alluvial fan, Fig. 8a) suggests that the Barskaun and Tamga Rivers remained near the top of the $Q_{III}^2$ fill until well into the subsequent deep lake regression. This occupation of the surface must have occurred over a long enough period to allow migration of flow over nearly the entire surface, leaving only isolated remnants of the original aggradational surface like the sampled location, which lies in the protected lee of the older $Q_{III}^1$ terrace outcrop. The offshore continuation of the $Q_{III}^2$ alluvial fan in the bathymetry also argues for the river maintaining a relatively static profile until well into the regression.

*3.2.3. Jety Oguz River*

The greatest number of terraces in the Issyk-Kul basin are preserved above the Jety Oguz River in the 11 km between the basement unconformity and the rangefront (Fig. 9a). The rangefront at Jety-Oguz is defined by the intersection of an exceptionally broad and well-preserved north-dipping $Q_{II}$ surface and the low-gradient floor of the modern Issyk-Kul basin. North of the rangefront, the river runs on the top of basin sediments.

The $Q_{II}^2$ terrace is the most prominent terrace in the vicinity of the Jety Oguz River (Fig. 9a). This terrace is highly planar and extends for 20 km along-strike to the east (Fig. 10a). The topographic surface of this $Q_{II}$ terrace does not exhibit a fan shape and cannot be clearly associated with deposition from any individual modern streams. West of the Jety Oguz River, the $Q_{II}$ surface is locally visible, but it has been cut by numerous minor fault scarps (the most clear examples are mapped on Fig. 9a) and more thoroughly dissected by gullies. Several $Q_{II}$ sublevels with southward-increasing separation are inset into the main surface in the Jety Oguz River canyon near the rangefront. Generally, the thicknesses of the Jety Oguz terrace

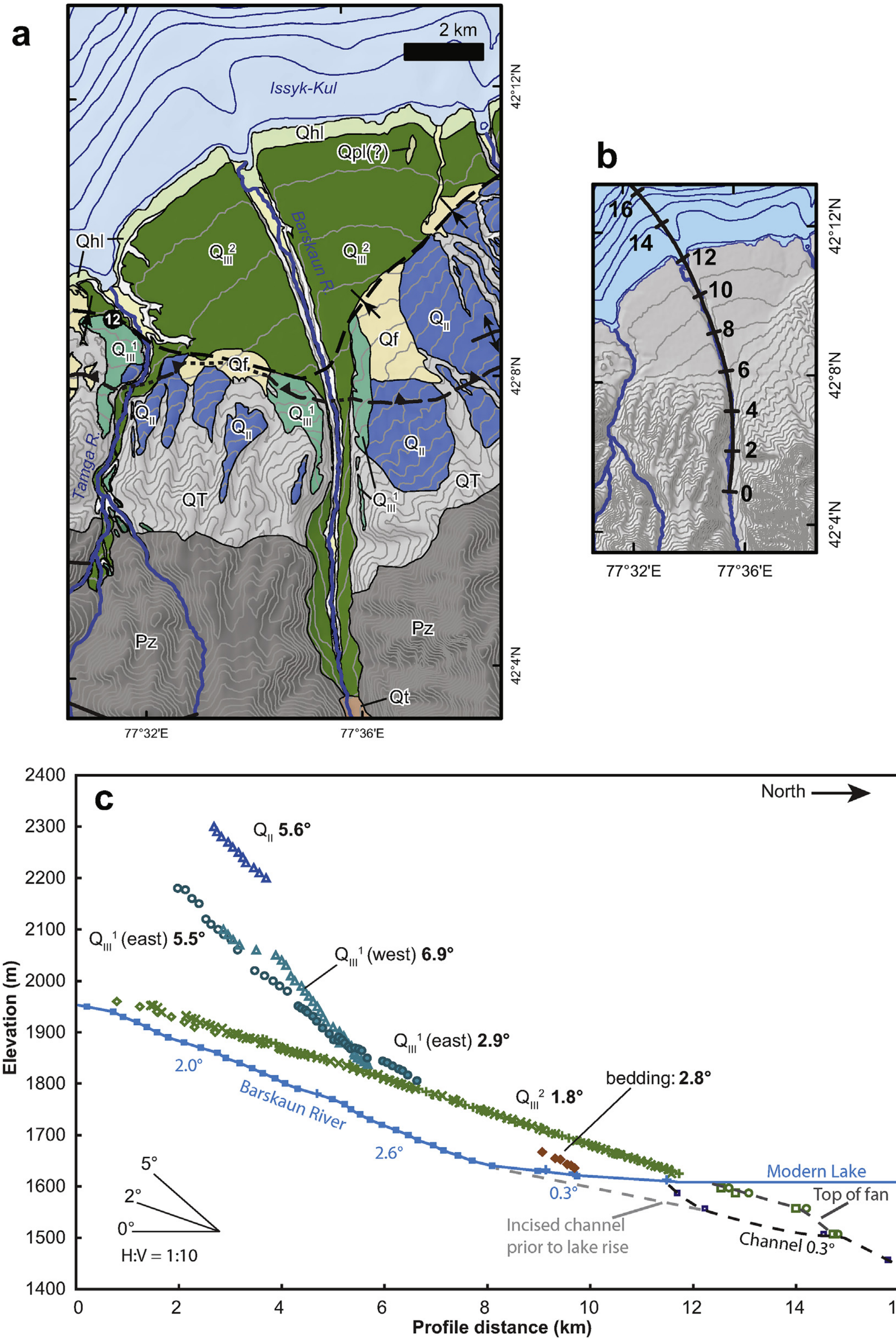


**Fig. 8.** (a) Quaternary geology and terraces along the Barskaun and Tamga rivers. The extensively $Q_{III}^2$ fan is graded to the lowest well-preserved moraines, and is locally dated by radiocarbon west of the Tamga River. See Fig. 5 for legend. (b) Profile line with distance (km). (c) Elevation profile of modern Barskaun River and terraces above. Solid, ‘x’, and ‘+’ symbols were surveyed with differential GPS, and open symbols digitized from topographic and bathymetric maps based on field mapping. The well-preserved $Q_{III}^2$ terrace is graded to a sub-lake fan. The modern river has a complicated profile due to incision and lake level fluctuation since the abandonment of the $Q_{III}^2$ terrace.

gravels are poorly defined, as the lower contacts of the terrace gravel with the coarse-grained Neogene sediment are poorly exposed on the vegetated risers. However, on the steep canyon walls near the southern limits of the upper $Q_{II}$ surfaces, there are

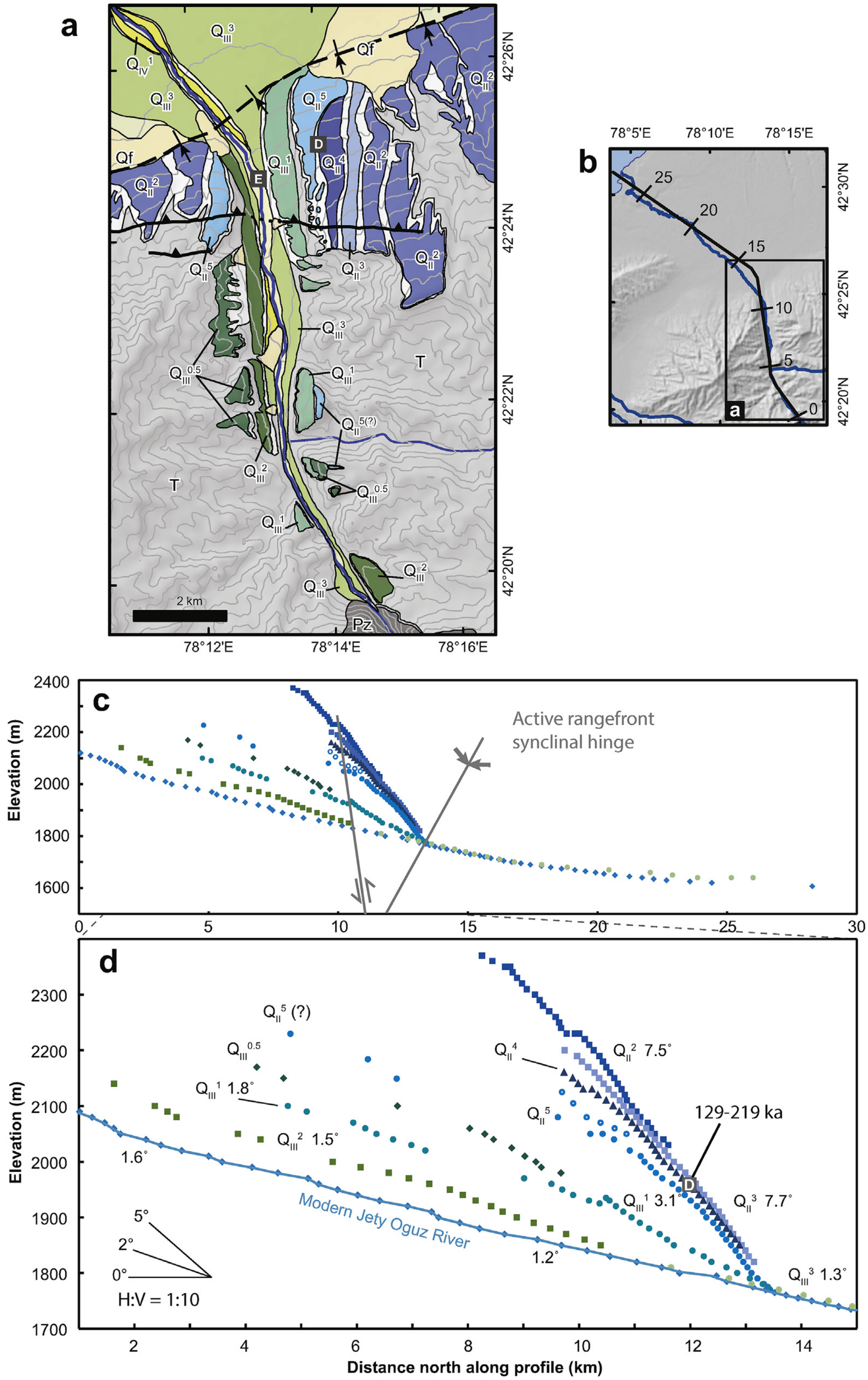


**Fig. 9.** (a) Late Quaternary river terraces along the Jety Oguz River. A well preserved, broad $Q_{II}^{2}$ surface caps the rangefront along this portion of the eastern Issyk-Kul basin, and multiple levels of $Q_{III}$ terraces are preserved along the modern river canyon. See Fig. 5 for legend. (b) Location of profile line, showing distance (km) and extent of Fig. 9b. (c) Long elevation profile of terraces along the Jety Oguz River and locations of active structures. (d) More detailed portion of profile with terrace names and angles indicated. North-dipping terrace remnants intersect at the rangefront and show a consistent pattern of steepening with age.

maximum thicknesses of 10–20 m of gravel overlying Neogene sediment. As the vertical separations between the different $Q_{II}$ levels are greater than the gravel thicknesses for the upper $Q_{II}$ terraces, the gravel of the inset terraces was most likely deposited sequentially between incision events, (as opposed to multiple cut surfaces developed on a single fill). Exposure of colluvial/aeolian deposits at the outer edge of the $Q_{II}^2$ terrace remnants show there is generally <5 m of sediment overlying the gravel surface except against north-side-up fault scarps and infilled gullies cut into the gravel surface.

Five distinct $Q_{III}$ terraces are inset below the extensive $Q_{II}$ surface. The $Q_{III}$ terraces are generally unpaired except for the $Q_{III}^3$ terrace, which is only a few meters above the modern river level at the rangefront, and connects to a large fan-shaped surface north of the rangefront. In the canyon, $Q_{III}$ terrace gravel deposits are covered by thick (10–50 m) accumulations of cover material shed from outcrops of weakly indurated Neogene sedimentary rock exposed in the risers above. The gravel/colluvium contacts of the higher $Q_{III}$ terraces are generally distinct as a marked, continuous color contrast even across vegetated hillsides (Fig. 10b), which permits easy tracing of terrace levels up the river valley. In cliff faces, where the basal gravel contacts of the $Q_{III}^1$ to $Q_{II}^5$ terraces are completely exposed, there is generally 5–10 m of fluvial gravel overlying strath surfaces, showing that periods of aggradation punctuated the overall trend of incision for the Jety Oguz River. The most prominent terrace is the $Q_{III}^1$ along the east wall of the Jety Oguz canyon, which is graded to remnants of a broad, upland low-relief surface. This morphology of $Q_{III}^1$ is similar to that in three river canyons immediately to the west, where $Q_{III}^2$ is clearer, and thus the position of $Q_{III}^1$ is more easily recognized.

*3.2.3.1. Jety Oguz profiles.* The striking feature of the Jety Oguz River terrace profiles is the convergence of the terraces and river north toward the rangefront (Fig. 9c and d). The modern Jety Oguz River has a linear to slightly concave profile in the canyon. North of the rangefront, the modern river slope declines progressively to <0.1° near its mouth (Fig. 9c). The $Q_{III}^3$ surface diverges from the river ~10 km upstream of the lake, merging with low gradient lake and other basin deposits. We did not map the Quaternary geology downstream of the rangefront in detail, and the $Q_{III}^3$ profile data of Fig. 9c are taken from the geomorphic surface, and thus may not exactly represent the actual top of the terrace gravel.

The river terraces show a consistent pattern of increasing gradient with relative age, particularly in the 3–6 km south of the rangefront (Fig. 9d). South of this zone, all of the $Q_{III}$ terraces are parallel with, or just slightly steeper than, the modern river. $Q_{III}^1$, the best preserved of these river terraces, shows an abrupt steepening across the north-side up fault that crosses the canyon. The $Q_{II}$ terraces show a steep northward slope over their entire outcrops, which generally terminate south of the fault, but north of the change in gradient for the $Q_{III}^{0.5}$ terrace (Fig. 9d). Similar to $Q_{III}^1$, all of the $Q_{II}$ terraces east of the river have steeper slopes north of the fault offset (6.8°–7.7°) and lower slopes to the south (4.5°–6.3°). The dips of the terrace segments on either side of this fault systematically increase with terrace age. The only possibly $Q_{II}$ age terrace preserved in the canyon is the terrace mapped as $Q_{II}^5$, but a 3 km gap between outcrops makes this correlation uncertain. There has been a minimum of ~500 m incision below the $Q_{II}^2$ terrace near its southern preserved extent.

*3.2.3.2. Jety Oguz chronology.* We sampled the $Q_{II}^4$ terrace east of the Jety Oguz River for $^{10}$Be profile dating ~10 m east of the top of the riser to the $Q_{II}^5$ terrace below (Fig. 9). Fine-grained sediment overlies a gradational contact with the gravel, and the $^{10}$Be concentration follows a well-defined exponential relationship with depth (Fig. 6b). We exclude the uppermost-analyzed sample because it appears to be primarily sand transported by aeolian or slope wash processes, and take the top of the gravel to coincide with top of the clast-supported sediment, sampled at 45 cm. The lowest sample has a large relative error and we exclude it from the regression analysis, using five samples (Fig. 6b).

We determine an absolute minimum $^{10}$Be depth profile age for the $Q_{II}^4$ terrace of 129 ± 14 ka by using the unshielded intact gravel as a limiting case (Fig. 6b). Using the scenario of the present covering sediment geometry having been present since the time of the terrace abandonment yields an age estimate of 219 ka, assuming a cover sediment density of 1.8 g/cm$^3$. We use a greater density than at Ak-Terek due to the greater concentration of large clasts incorporated in the cover sediment. This provides a maximum limiting age for the likely scenario of the cover sediment monotonically increasing in thickness through time. The $^{10}$Be concentration at the lowest sampled depth of 230 cm is 7% of that at the top of the profile, similar to the estimated $^{10}$Be production rate at this depth (Table 2). This coupled with the low $^{10}$Be concentration of the modern Jety Oguz River sand (~1% of the upper profile concentration) suggests a negligible inherited contribution

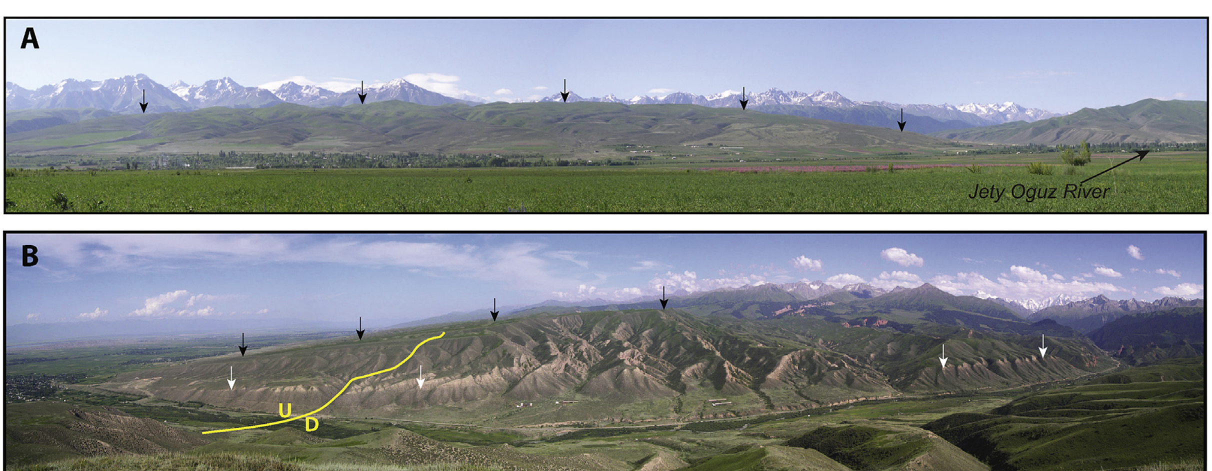


**Fig. 10.** Panoramas of Jety Oguz terraces. (a) View south from basin floor to the expansive north-dipping planar $Q_{II}^2$ surface (upper extent noted with arrows). (b) View to east across Jety Oguz River. Black arrows show top of $Q_{II}^2$ terrace, the white arrows point to the gravel/cover contact for $Q_{III}^1$.

to the age (Table 2). Progressive growth of the cover sediment is supported by the relatively low concentration of $^{10}$Be from the sample within the cover. Using end-member shielding scenarios to bracket the history of the 22 cm of sediment presently overlying this sample returns an age range of 184 to 142 ka. With only a single sample we cannot define the inherited $^{10}$Be concentration for the cover, but we favor the interpretation that the present cap was deposited ~180 ka, which supports the older end of the age range we calculate for the gravel.

## 4. Discussion

### *4.1. Synthesis of Issyk-Kul terrace history*

We integrate the data from the locations presented here, our other observations (Burgette, 2008), and previous work (Section 1.2) to synthesize a history of terraces in the Issyk-Kul basin. Our data for terraces older than $Q_{III}^{2}$ place broad constraints on the timing of formation. The best data are from the Ak-Terek River, where $^{10}$Be profile ages give estimates for the timing of the formation of two pre- $Q_{III}^{2}$ terraces with $Q_{III}$ morphologies. Roughly equal amounts of incision and tectonic deformation in the intervals between the abandonment of $Q_{III}^{1}$ and earlier $Q_{III}^{0.5}$ and later $Q_{III}^{2}$ are consistent with the approximately equal intervals derived from the $^{10}$Be dating (Fig. 7). The numerical ages suggest the major terraces formed on a cycle with a period of ~100 ka over the past 300 ka (Fig. 11).

The late Pleistocene highstand of Issyk-Kul was an important event in the most recent river terrace-forming cycle (the past ~ 120 ka). Based on radiometric age and field relationships, Lake Issyk-Kul rose above its modern sill at about 43 cal ka BP or slightly earlier, and reached a highstand ~33 m above the modern sill by ~25 cal ka BP (Fig. 12). Based on the geometry and chronology of the lake deposits, the sill for this highstand must have been downstream of the western Issyk-Kul basin, in Boam Canyon. One possible source of the dam is a landslide in the gorge. Alternatively, the sill may have grown through colluvial sedimentation in the gorge while the Chu River was routed into a closed, low standing Lake Issyk-Kul. Once this high sill was breached post-25 cal ka BP, the Chu River likely re-occupied its modern route west of Lake Issyk-Kul, and the closed lake experienced a regression of 50–100 m below present (Fig. 12). The lake subsequently filled back to overflow levels in the latest Holocene, based on our dates and historical accounts (Ricketts et al., 2001).

The development of $Q_{III}^{2}$ terraces is much better defined than the older terraces, and is generally consistent for all of the river valleys along the southern margin of Issyk-Kul. The earliest event in the relative chronology for the construction of $Q_{III}^{2}$ is a preceding interval of incision and valley widening greater than the Holocene. Even along reaches where preserved higher terraces show a clear trend of fluvial incision over the late Quaternary, the base of the $Q_{III}^{2}$ fill is not exposed in the modern inner gorges. The base of the $Q_{III}^{2}$ fill is only exposed in the areas of the highest rock uplift rates, such as near anticlinal hinges along the Ak-Terek River and the southernmost terrace remnants along the northward-tilting Jety Oguz area. One possible cause of such deep incision is a more extreme lake regression than the 50–100 m below modern level regression documented for the early Holocene (e.g., Zabirov et al., 1973; Gebhardt et al., 2016). The bathymetry of Issyk-Kul has low gradient areas >150 m below the modern sill that have been interpreted as terraces (De Batist et al., 2002). Seismic reflection data have also been interpreted as showing deposition of deltaic sediment over 400 m below the modern lake level (Gebhardt et al., 2016).

Radiocarbon ages near the top of the $Q_{III}^{2}$ fill and interfingering

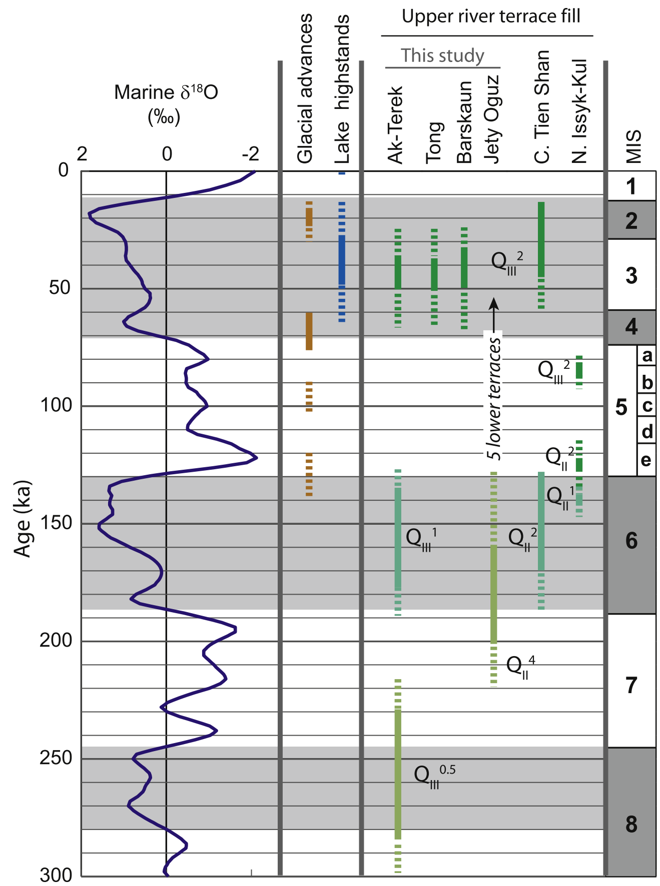


**Fig. 11.** Correlation of Issyk-Kul river terrace formation with terrace chronologies from the central Kyrgyz Tien Shan (Thompson et al., 2002) and Toru Aygir River, northern Issyk-Kul (Selander et al., 2012). Terrace names are as mapped locally. Timing of Issyk-Kul lake high stands is based on our observations. Timing of glacial advances from dated moraines in the Kyrgyz Tien Shan (Koppes et al., 2008; Narama et al., 2007; Zech, 2012; Lifton et al., 2014a; Blomdin et al., 2016), and global climate from a marine oxygen isotope compilation (Imbrie et al., 1984). Gray bands show times when global curve shows greater than average $\delta^{18}$O values (times of greater global ice volume). MIS column indicates marine oxygen isotope stages. Generally, the current set of dates from the top of the $Q_{III}^{2}$ fill from Kyrgyz Tien Shan terraces is consistent with synchroneity of aggradation. Major aggradational terrace forming events for older terraces appear to have occurred once per global glaciation, although the morphologic correlations do not match the numerical dating correlation.

older lake beds are consistently >40 cal ka BP, near or beyond the limits of radiocarbon. Given the very low $^{14}$C concentrations and stratigraphic positions of the samples in the upper part of the fill, our radiocarbon ages place little constraint on the initiation or duration of the $Q_{III}^{2}$ fill, (e.g., >100 m thickness at the Barskaun River). The top of the $Q_{III}^{2}$ fill was at least locally abandoned near the edges of the river valleys by 38–37 cal ka BP, based on the oldest ages from cover sediment on $Q_{III}^{2}$ at the Ak-Terek and Barskaun Rivers. The $Q_{III}^{3}$ cut/strath terrace at Ak-Terek is inset only ~5 m below the top of the $Q_{III}^{2}$ gravel where we dated the cover wedge on $Q_{III}^{2}$ (Fig. 5d); however, this terrace post-dates the termination of the late Pleistocene lake highstand (<25 ka) 5 km downstream at the Ak-Terek mouth. Likewise, the $Q_{III}^{2}$ alluvial fan at the mouths of the Barskaun and Tamga rivers appears to have been maintained near its upper surface until regression of the lake below the modern sill. Based on Thompson et al. (2002), deeper incision likely occurred ~ 15–13 cal ka BP.

Field relationships at Ak-Terek show that deposition of the $Q_{III}^{2}$ gravel overlapped in time with deposition of the higher lake deposits above the modern sill elevation. However, the continuous

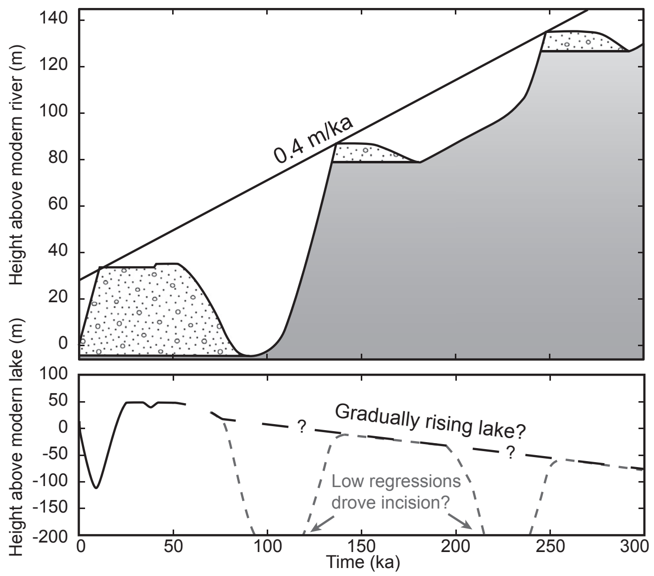


**Fig. 12.** Speculative history of the Ak-Terek River and Issyk-Kul, constrained by the available chronological data for major terraces. River incision figure is after Bull (1991). Particularly for the $Q_{III}^{2}$ terrace, the major incision through the fill lags well after the end of aggradation. The deep fill under the $Q_{III}^{2}$ surface appears to follow an unusually deep incision event, which was potentially caused by a low regression of the lake.

morphology of the exposed river terraces and now-underwater fans at the mouths of every river we studied argue that the $Q_{III}^{2/3}$ rivers maintained the same gradients upstream of the modern shoreline during the ~100 m lake regression, likely linked with downstream growth of the now submerged fans and deltas.

Following aggradation of the fans below the modern lake level, all of the rivers incised canyons through the $Q_{III}^{2}$ fill. The underwater canyons appear graded to the slopes of the modern rivers upstream of the local concave reaches near the modern mouths. This incision may have been driven by a climatic change in the sediment to transport capacity ratio of the rivers, or propagation of knickpoints that formed when the lake level dropped to levels that exposed lake floor with a steeper gradient than the alluvial slope of the fans and deltas. The first possibility is supported by the pattern of synchronous post-$Q_{III}^{2}$ deep incision in the basins to the west, which do not have lakes (Thompson et al., 2002). The lack of detailed lake history and climatic information for the period of latest Quaternary Issyk-Kul regression prevents us from more directly assessing the timing and cause of the fan incision.

The late Holocene high stand of Issyk-Kul at the modern sill elevation caused adjustments in the gradients of the lower reaches of the rivers. The low gradients of the northern 3–4 km of the rivers and the sublacustrine channels immediately offshore interrupt the otherwise linear profiles of the modern rivers and underwater extensions (Figs. 5c and 8c). This morphology reflects deposition of a wedge of sediment in response to the baselevel rise.

### *4.2. Correlation with other Kyrgyz Tien Shan terraces and glaciations*

The fluctuation of lake levels likely influenced the history of southern Issyk-Kul rivers, but the morphologic correlations and available numerical age constraints are generally consistent with rivers in the central Tien Shan to the west having histories of aggradation and incision that were broadly synchronous with those of Issyk-Kul rivers (Fig. 11). Along rivers in three basins to the west that do not have lakes, $Q_{III}^{2}$ fill terraces form prominent surfaces that were abandoned ~15.7–13.5 cal ka BP, and incised by narrow modern gorges (Thompson, 2001; Thompson et al., 2002). In the Naryn basin, charcoal leaves from the middle of the alluvial fill of the Kajerty River $Q_{III}^{2}$ terrace yielded ages of ≥43 ka BP (Thompson, 2001). On the north side of Issyk-Kul, a surface mapped as $Q_{III}^{2}$ yielded age estimates of 85.6 ± 7.6 ka and 105–57 ka using TCN and luminescence dating, respectively (Bowman et al., 2004b; Selander et al., 2012). Similar to our data from southern Issyk-Kul, this suggests the $Q_{III}^{2}$ strath and much or the entire fill were developed early in the last glacial cycle. The age from the uppermost portion of the gravel shows that the Kajerty River was at the top of its fill at ~14 cal ka BP, in contrast to the Issyk-Kul rivers that subtly incised below the top of the $Q_{III}^{2}$ fill prior to 35 cal ka BP. However, the dated samples at the Kajerty River were collected near the modern river and distant from the riser to the terrace above, so while incision is well defined locally, most of the fill may have been deposited earlier and the river had remained near the top of the fill until the deep incision occurred. Ages from $Q_{III}^{3}$ terraces below the $Q_{III}^{2}$ surfaces are indistinguishable from the main $Q_{III}^{2}$ surface, suggesting that incision proceeded relatively rapidly (Thompson, 2001). Another difference between the Issyk-Kul river terraces and those from the central Kyrgyz Tien Shan is presence of an early to middle Holocene $Q_{IV}^{1}$ terrace associated with most of the rivers studied by Thompson (2001). The general lack of this terrace in the Issyk-Kul basin likely reflects the incision of the Issyk-Kul streams below the modern base level in response to the regression of the lake during the early Holocene.

The ages of Issyk-Kul river terraces are consistent with the timing of regional glaciation and suggest the end of aggradation is temporally decoupled from the timing of significant incision. Although the age control leaves uncertainty regarding the timing of accumulation of the $Q_{III}^{2}$ gravel, there is strong evidence for aggradation being largely complete prior to the global last glacial maximum (as defined by Clark et al. (2009) during marine oxygen isotope stage [MIS] 2 at ~ 26–19 ka). The uppermost fill was also at least locally abandoned ~20 ka prior to the likely timing of deep incision (16–13 ka) during the most recent global glacial-interglacial transition at ~ 19–10 ka (Thompson et al., 2002, Fig. 11). The 16–13 ka river incision dated by Thompson et al. (2002) slightly precedes the ~12.5 ka age of the most extensive late Quaternary deglaciation in the Tien Shan (Takeuchi et al., 2014). Hence, the start of aggradation of the $Q_{III}^{2}$ gravel is likely linked to the most prominent latest Pleistocene glaciation in the Tien Shan. The emerging ages of glacial features throughout the Tien Shan suggest that the largest latest Pleistocene glacial advance occurred during MIS 4 (60–80 ka) rather than during the most recent global ice volume maximum of MIS 2 (Abramowski et al., 2006; Narama et al., 2007, 2009; Koppes et al., 2008; Zhao et al., 2010; Zech, 2012). More rapid accumulation of loess in the northern Tien Shan during MIS 2 relative to the rest of the late Quaternary has been interpreted to reflect arid conditions during MIS 2, supporting previous inferences from studies of glacial chronology (Youn et al., 2014).

Studies from the Terskey Range are conflicting with regard to the extent of glaciation during MIS 2, with the $^{10}Be$ exposure dating study of Koppes et al. (2008) finding no evidence of advance far beyond the limits of modern glaciers, and the OSL dating studies of Narama et al. (2007, 2009) yielding multiple dates in the 29–21ka range on moraines only ~ 350 m above the elevations of the MIS 4 terminal moraines. TCN studies of moraines associated with the highest peaks southeast of the Terskey Range found prominent MIS 2 age moraines with elevations consistent with more moderate advance of glaciers and evidence of more extensive pre-MIS 2 glaciers (Lifton et al., 2014a; Blomdin et al., 2016). Although there are no published ages of the lowest moraines in the Barskaun valley, the $Q_{III}^{2}$ terrace is graded to the lowest preserved moraines.

This field relationship suggests that aggradation of the $Q_{III}^{2}$ gravel was related to the 80–70 ka local maximum glacial advance and subsequent glacial interval. The association of late Pleistocene terminal moraines and outwash terraces is widely observed in other mountainous landscapes (e.g., Reheis et al., 1991; Pinter et al., 1994; Chadwick et al., 1997). Increased sediment production related to larger glacial extent is observed in modern landscapes (Hallet et al., 1996), and increased sediment flux into river systems provides a likely explanation for the aggradation.

Guided by the inferences from $Q_{III}^{2}$ linking the start of aggradation to the local last glacial maximum (~80–60 ka) and deep incision to the global deglacial transition, we can better assess our numerical ages for the older river terraces. Although uncertainties regarding the cover sediment history make the error bars broad, the robust minimum age limit for the $Q_{III}^{1}$ terrace suggests its aggradation occurred prior to the MIS 5e interglacial (Fig. 11). The minimum age for the higher $Q_{III}^{0.5}$ surface indicates deposition prior to the MIS 7 interglacial. These broad chronometric constraints, coupled with the evidence that such terrace fills form during periods of glaciations, suggest that the three recent major Ak-Terek terrace levels formed during each of the last three global glaciations. Apparent asynchrony of the latest Pleistocene glacial advances in the Tien Shan with respect to the global ice volume history (Koppes et al., 2008; Narama et al., 2009; Lifton et al., 2014a) preclude us from confidently making greater refinements of the terrace ages based on global climate records. The global climate regulation of terrace forming events is also supported by the approximately equal amounts of incision and deformation that occurred between $Q_{III}^{1}$ and the terraces above and below (Fig. 7). The MIS 6 age of formation for $Q_{III}^{1}$ terrace at Ak-Terek may correlate with terraces that have $Q_{II}$ morphologies along rivers in the central Kyrgyz Tien Shan dated by Thompson et al. (2002; Fig. 11). Their luminescence ages for sediments capping a terrace mapped as $Q_{II}^{2}$ give a best estimate of terrace abandonment at 140.7 ± 8.5 ka, assuming synchronous incision occurred in three basins.

The situation at Jety Oguz, where we dated the $Q_{II}^{4}$ terrace, is more complicated to resolve. The uncertainty age range of this terrace (219–129 ka) results from the relatively thick cover sediment at the sampled site. Based on the geochronology, the Jety Oguz $Q_{II}^{4}$ would correlate with the $Q_{III}^{0.5}$ terrace at Ak-Terek, and many of the other Jety Oguz terraces would represent more minor terraces that were not formed or preserved in other areas. Alternatively, the $Q_{II}^{4}$ terrace could be older than the sequence we dated at Ak-Terek. In the context of the total ~0.5 km incision of the Jety Oguz River, the dated $Q_{II}^{4}$ terrace is inset only subtly into the expansive $Q_{II}^{2}$ surface. The broad extent of the $Q_{II}^{2}$ terraces in both the eastern and western Issyk-Kul areas suggests a fundamental difference in the geomorphic system during their development compared to the more recent terraces, perhaps driven by a common climatic regime. At Ak-Terek, the slope of the $Q_{II}$ surface is approximately three times that of the $Q_{III}^{1}$ terrace after accounting for the initial slope from the regression shown in Fig. 7. If the deformation rate and style has remained constant, the age of the $Q_{II}$ surface would be in the ~750 ka range. The expansive $Q_{II}^{2}$ terrace at Jety Oguz (Figs. 9 and 10) is the seventh to ninth major terrace above the river, and if there is one major terrace per ~100 ka glacial cycle, the $Q_{II}$ surfaces could correlate along the entire basin. In this case, the much younger age from the Jety Oguz $Q_{II}$ surface could result from the sampled location having had a thicker cover over much of its history. A time-averaged thickness of ~60–100 cm greater than modern cover thickness would explain the discrepancy (depending on the overlying sediment density and age difference between $Q_{II}^{2}$ and $Q_{II}^{4}$). In this case the switch in the nature of terrace formation would coincide with the ~800 ka mid-Pleistocene transition from ~40 ka to ~100 ka glacial cycles (e.g., Pisias and Moore, 1981; Ruddiman et al., 1986). The more rapid climatic oscillations of the earlier Pleistocene may have promoted broad planation rather than deep valley entrenchment (Bridgland and Westaway, 2008). However, if accumulation of sediment at the sampled Jety Oguz $Q_{II}^{4}$ site has been monotonic and the age is correct, the conditions required for very broad planation must have been caused by more local factors that caused the generation of similar terrace morphologies in different parts of the Issyk-Kul basin at different times. Future dating of additional terrace levels at Jety Oguz and elsewhere would resolve which possibility is more likely.

### 4.3. Inferred controls on the terrace forming process

The general temporal link we find between alluvial aggradation during glaciation in headwaters areas and incision during deglaciation matches inferences made in previous studies of terraces in the Kyrgyz and Chinese Tien Shan (Molnar et al., 1994; Thompson et al., 2002; Poisson and Avouac, 2004; Lu et al., 2010) as well as many other mountainous areas elsewhere. However, the relatively well-dated history of southern Issyk-Kul $Q_{III}^{2}$ terraces shows a different pattern of terrace development than previously inferred. In the conceptual model of Bull (1991), the switch from gravel aggradation to incision represents a threshold process, in which rivers switch relatively quickly from aggradation to deep incision back to the tectonically-controlled base level. Guided by this idea, one would expect the age for the uppermost surface of an aggradational deposit to be relatively close to the age of incision below it. Owing to the difficulty in getting multiple ages through a sequence of aggradational and degradational events to truly define the rates of these processes, there are few studies that offer good constraints for fill terrace deposits. Weldon (1986) used radiocarbon ages from within and above fill terrace deposits along Cajon Creek in southern California to show that a pulse of aggradation migrated upstream through time, with the peak fill closely followed by a switch to down-cutting. Pederson et al. (2006) obtained multiple ages from late Quaternary aggradational events along the Colorado River in the Grand Canyon, from which they interpreted fairly rapid switches from aggradation to incision.

Our data from the southern Issyk-Kul rivers show a different situation, where the river aggraded to the top of $Q_{III}^{2}$ and then remained near that level for a period of at least ~10 ka, and likely >20 ka (Fig. 12). This suggests that the rivers maintained a quasi-equilibrium long profile in spite of long-term tectonically-induced base level fall. Perhaps the tectonic base level fall was in part balanced by base level rise to the late Pleistocene high stand of the lake, but it motivates careful dating of incision and aggradation events in this and other regions.

### 4.4. Implications for tectonic geomophology and neotectonics

#### 4.4.1. Terrace correlation

Our numerical ages for terraces coupled with previous work, allow us to test the effectiveness of intra- and inter-basin terrace correlations made in the Kyrgyz Tien Shan on the basis of distinctive geomorphology. The set of numerical ages suggests that the terrace associated with the youngest significant aggradational event is correctly correlated as $Q_{III}^{2}$ around our study areas in the Tien Shan. The correlation is robust in spite of the $Q_{III}^{2}$ surface having a strath terrace morphology in places of higher uplift rates and being a fill terrace in other locations. The generally complete preservation of this latest Pleistocene terrace allows us to trace the top of the terrace gravel from locations with thin fluvial deposits into areas of thicker fill. Merritts et al. (1994) show that longitudinal variations in terrace character result from proximity to a fluctuating base level control as well. These observations motivate cautious use of strath versus fill morphology as a correlation tool and careful longitudinal tracing of terraces in areas with discontinuous outcrops.

For terraces from the penultimate aggradational cycle, terrace correlations are more dependent on the preservation of terraces associated with particular rivers. The inter-basin terrace mapping in the central Kyrgyz Tien Shan by Thompson et al. (2002) is supported by consistent numerical ages of the abandonment of what was mapped as the $Q_{II}^{2}$ terrace. However, along the rivers they studied, there were only two major levels of terraces with similar extensive morphologies. The mapped outcrop widths of the $Q_{II}^{2}$ terraces are similar to those of the $Q_{III}^{2}$ terraces, and the $Q_{II}$ terraces do not appear to cap the topography to the extent of those from the Issyk-Kul basin. The Kyrgyz terrace correlation scheme, at least as applied here, involves identifying the two most prominent terraces and calling them $Q_{III}^{2}$ and $Q_{II}^{2}$, with the $Q_{II}^{2}$ surface near the local topographic culminations. The remaining terrace names are then interpolated between the major levels. As a result, the potential for miscorrelation is high if there are major variations in incision rates and the associated removal of uplifted terraces by erosion. If only the $Q_{III}^{2}$ and $Q_{III}^{1}$ terraces west of the Ak-Terek River were currently preserved, we would have correlated the terrace flight in a different fashion, and comparison to incision rates from the rivers of the central Kyrgyz Tien Shan would be more straightforward.

The number and ages of terraces that survive along a given river is controlled by the pattern of river migration and lateral erosion following terrace abandonment. Terrace preservation and pairing is analogous to the problem of moraine preservation (Gibbons et al., 1984), and a consistent migration direction of a river or progressive valley narrowing promotes preservation of long terrace sequences. Preservation of the three major levels of late Pleistocene terraces along the Ak-Terek River from the last 300 ka was promoted by a net eastward migration of the river and the greater erosional resistance of the terrace gravel in comparison to the underlying late Cenozoic mudstones. The $Q_{III}^{1}$ and $Q_{III}^{0.5}$ terraces are unpaired, so we cannot assess how much wider the paleo-floodplains were at the time of terrace abandonment. The morphological distinction of terrace pairing has been used to identify climatically-controlled terraces (Bull, 1991; Merritts et al., 1994). However, the $\geq$10 m of gravel overlying the bedrock straths, and the lack of discernable cross-valley slope argue for the $Q_{III}^{1}$ and $Q_{III}^{0.5}$ Ak-Terek terraces representing major climatically-controlled events. The migration of the Ak-Terek River up-plunge relative to active structures was likely promoted by the inverted relationship between gravel and "bedrock" erodibility (Burgette, 2008).

### *4.4.2. Initial terrace slopes*

Understanding the initial slope of terraces at the time of abandonment is key to using deformed terraces as quantitative markers of angular deformation. Most studies assume that the down-valley slope of the modern river provides the best estimate of the initial terrace geometry as well (e.g., Thompson et al., 2002; Amos et al., 2007). This assumption is likely valid in many cases when comparing a strath terrace to a modern river that is in a period of lateral planation across bedrock. Observations of differences in slope between aggrading and incising rivers suggest caution in making such comparisons between terraces and rivers in different stages of the terrace forming cycle (Leopold and Bull, 1979; Merritts et al., 1994). Another example of non-parallelism between a modern river and an initial terrace slope occurs when the modern river profile is in a transient state due to localized incision via knickpoint migration or local aggradation (e.g., Weldon, 1986). In addition to biasing estimates of tilting, non-parallelism between terraces and the modern stream profile will make calculations of incision rate vary longitudinally along a river. This effect adds to the temporal biases others have noted in calculating incision rates from terraces and rivers that are in different states of development (e.g., Gardner et al., 1987; Hancock and Anderson, 2002; Gallen et al., 2015).

Terrace and river profiles from the southern Issyk-Kul rivers illustrate all of these issues related to estimating incision and deformation. There are local concavities near almost every river mouth due to relatively recent lake level rise and the resultant aggraded wedges of sediment. Local convexities in the modern river profiles exist along both the Ak-Terek and Barskaun Rivers, related to either lithologic constrasts and/or transient incision patterns. Converting terrace profiles into height above the modern river would produce spurious curvature in terraces along these reaches that could be falsely attributed to tectonic deformation, especially in locations with more subdued signals. Although there is question whether an aggradational alluvial surface can be truly considered graded and in equilibrium (Phillips, 1991; Muto and Swenson, 2005), the consistent linearity of the terrace profiles suggests that the terraces represent a more ordered, stable geometry than the transient condition of the lower parts of the modern rivers.

The best evidence we have that the upper surfaces of the Issyk-Kul river terraces were formed with an essentially consistent gradient, especially in comparison to the curved modern river, comes from the Ak-Terek River (Fig. 5d). Long profiles of the three major late Pleistocene terraces are highly linear, and the consistent northward tilting of the Neogene sediment, the $Q_{II}$ terraces, and the $Q_{III}$ terraces gives a well-resolved tectonic forcing. The consistent slope-age relationship shown in Fig. 7 suggests the terraces formed at an initial slope of ~0.6°. An ambiguity for the older terraces remains in that the uppermost surface of the $Q_{III}^{2}$ deposit has a <0.1° lower slope than the younger cut $Q_{III}^{3}$ surface. The $Q_{III}^{1}$ and $Q_{III}^{0.5}$ gravel surfaces could represent either the top of the fill, analogous to $Q_{III}^{2}$, or a cut surface planed across the fill in a time of relative stability such as the $Q_{III}^{3}$ surface.

## 5. Conclusions

Our observations of the geology and chronology of terraces in the southern Issyk-Kul basin contribute to the understanding of process and timing of terrace formation in the Kyrgyz Tien Shan. Our numerical dating tests the Soviet-era correlation scheme, and we find that identification of the youngest major aggradational terrace ($Q_{III}^{2}$) is likely correct in most cases. This terrace aggraded during and after the peak in the last major glaciation of the Tien Shan (~80–60 ka), which preceded the last global ice-volume maximum at 26–19 ka (Clark et al., 2009). This asynchrony between regional and global climate records illustrates the potential for major uncertainty by simply applying the global Quaternary climate curves to specific flights of fluvial terraces. Our $^{10}$Be ages on older terraces at Ak-Terek and Jety Oguz support the finding of Thompson et al. (2002) from the central Kyrgyz Tien Shan that there was one major aggradational terrace-forming event per ~ 100 ka glacial cycle, and that deep incision likely occurs during the major glacial-interglacial transitions. Although the few ages on terraces older than 50 ka support relatively synchronous aggradation and abandonment in the area, the terrace correlations we make based on radiometric dating are different in some cases than had been previously inferred based on morphologic criteria. Differential preservation of terraces between rivers and basins complicates accurately making relative correlations.

The presence of the large lake Issyk-Kul both aids and complicates deciphering the controls on river terrace development and abandonment. Our radiocarbon ages on lacustrine sediment at the elevation of the modern sill support historic accounts of outflow in the latest Holocene. Our ages for three sections of late Pleistocene lake sediment better quantify the duration of the high stand associated with the prominent shoreline from at least 43 cal ka BP to <25 cal ka BP. The overlapping age ranges from the sample in the Kok-Moynok basin and the sites on the south shore of Issyk-Kul suggest that most of the modern elevation of the Pleistocene shoreline above the Holocene sill was likely due to damming of the Chu River downstream of Issyk-Kul. Radiocarbon dates and geologic relationships between the lake and river terraces show that the southern Issyk-Kul rivers remained at or near the top of the $Q^2_{III}$ fill for 10–30 ka. This observation motivates a good understanding of the relationship between dated material and the offset landform when using terraces to quantify active tectonics.

## Acknowledgments

This work was supported by NSF grant INT-0209874. We thank students of the Tien Shan International Geologic Field Camp for assistance with fieldwork. Radiocarbon and cosmogenic nuclide dating was partially supported by grants from the Geological Society of America and the American Association of Petroleum Geologists. Thanks to Michele Koppes, Nicole Davis, and Jason Dortch for providing assistance with processing cosmogenic nuclide samples. Damien Delvaux provided the bathymetric DEM of Issyk-Kul from De Batist et al. (2002). We thank Josh Roering for helpful comments on an earlier version of this manuscript. We thank two anonymous reviewers for constructive comments that improved the clarity of this paper.

## References

Abdrakhmatov, K.Y., Aldazhanov, S.A., Hager, B.H., Hamburger, M.W., Herring, T.A., Kalabaev, K.B., et al., 1996. Relatively recent construction of the Tien Shan inferred from GPS measurements of present-day crustal deformation rates. Nature 384, 450–453.
Abdrakhmatov, K.E., Weldon, R., Thompson, S., Burbank, D., Rubin, C., Miller, M., Molnar, P., 2001. Origin, direction, and rate of modern compression of the Central Tien Shan. Geol. Geophys. Russ. 42, 1585–1609.
Abramowski, U., Bergau, A., Seebach, D., Zech, R., Glaser, B., Sosin, P., Kubik, P.W., Zech, W., 2006. Pleistocene glaciations of Central Asia: results from Be-10 surface exposure ages of erratic boulders from the Pamir (Tajikistan), and the Alay-Turkestan range (Kyrgyzstan). Quat. Sci. Rev. 25, 1080–1096.
Aleshinskaya, Z.V., Bondarev, L.G., Voskresenskaya, T.N., Leflat, O.N., 1971. Recent Fill of the Lake Issyk-Kul basin (In Russian). Moscow University Press, Moscow, 164p.
Amos, C.B., Burbank, D.W., Nobes, D.C., Read, S.A.L., 2007. Geomorphic constraints on listric thrust faulting: implications for active deformation in the Mackenzie Basin, South Island, New Zealand. J. Geophys. Res. Solid Earth 112, B03S11.
Anderson, R.S., Repka, J.L., Dick, G.S., 1996. Explicit treatment of inheritance in dating depositional surfaces using in situ Be-10 and Al-26. Geology 24, 47–51.
Arendt, A., Bliss, A., Bolch, T., Cogley, J.G., Gardner, A.S., Hagen, J.-O., et al., 2015. Randolph Glacier Inventory – a Dataset of Global Glacier Outlines: Version 5.0: Global Land Ice Measurements from Space. digital media, Boulder Colorado, USA.
Balco, G., Stone, J.O., Lifton, N.A., Dunai, T.J., 2008. A complete and easily accessible means of calculating surface exposure ages or erosion rates from $^{10}$Be and $^{26}$Al measurements. Quat. Geochronol. 3, 174–195.
Blomdin, R., Stroeven, A.P., Harbor, J.M., Lifton, N.A., Heyman, J., Gribenski, N., Petrakov, D.A., Caffee, M.W., Ivanov, M.N., Hättestrand, C., Rogozhina, I., 2016. Evaluating the timing of former glacier expansions in the Tian Shan: a key step towards robust spatial correlations. Quat. Sci. Rev. 153, 78–96.
Borchers, B., Marrero, S., Balco, G., Caffee, M., Goehring, B., Lifton, N., Nishiizumi, K., Phillips, F., Schaefer, J., Stone, J., 2016. Geological calibration of spallation production rates in the CRONUS-Earth project. Quat. Geochronol. 31, 188–198.
Bowman, D., Korjenkov, A., Porat, N., 2004a. Late-Pleistocene seismites from lake Issyk-Kul, the tien shan range, Kyrghyzstan. Sediment. Geol. 163, 211–228.
Bowman, D., Korjenkov, A., Porat, N., Czassny, B., 2004b. Morphological response to Quaternary deformation at an intermontane basin piedmont, the northern Tien Shan, Kyrghyzstan. Geomorphology 63 (1), 1–24.
Bridgland, D., Westaway, R., 2008. Climatically controlled river terrace staircases: a worldwide Quaternary phenomenon. Geomorphology 98 (3), 285–315.
Bronk Ramsey, C., 2009. Bayesian analysis of radiocarbon dates. Radiocarbon 51 (1), 337–360.
Burgette, R.J., 2008. Uplift in Response to Tectonic Convergence: the Kyrgyz Tien Shan and Cascadia Subduction Zone [Ph.D. thesis]. University of Oregon, Eugene, 242 pp.
Bull, W.B., 1991. Geomorphic Responses to Climatic Change. Oxford University Press, London, 326 pp.
Chadwick, O.A., Hall, R.D., Phillips, F.M., 1997. Chronology of Pleistocene glacial advances in the central rocky mountains. Geol. Soc. Am. Bull. 109, 1443–1452.
Chediya, O.K., 1986. Morphostructures and Neotectonism of the Tien Shan (In Russian). Frunze (Bishkek), Ilim, 313 pp.
Clark, P.U., Dyke, A.S., Shakun, J.D., Carlson, A.E., Clark, J., Wohlfarth, B., Mitrovica, J.X., Hostetler, S.W., McCabe, A.M., 2009. The last glacial maximum. Science 325, 710–714.
De Batist, M., Imbo, Y., Vermeesch, P., Klerkx, J., Giralt, S., Delvaux, D., Lignier, V., Beck, C., Kalugin, I., Abdrakhmatov, K., 2002. Bathymetry and sedimentary environments of lake Issyk-Kul, Kyrgyz republic (Central Asia): a large, high-altitude, tectonic lake. In: Klerkx, J., Imanackunov, B. (Eds.), Lake Issyk-Kul: its Natural Environment. Kluwer Academic Publishers, Dordrecht, pp. 101–123.
Gallen, S.F., Pazzaglia, F.J., Wegmann, K.W., Pederson, J.L., Gardner, T.W., 2015. The dynamic reference frame of rivers and apparent transience in incision rates. Geology 43 (7), 623–626.
Gardner, T.W., Jorgensen, D.W., Shuman, C., Lemieux, C.R., 1987. Geomorphic and tectonic process rates: effects of measured time interval. Geology 15, 259–261.
Gebhardt, A.C., Naudts, L., De Mol, L., Klerkx, J., Abdrakhmatov, K., Sobel, E.R., De Batist, M., 2016. An extended history of high-amplitude lake-level changes in tectonically active Lake Issyk-Kul (Kyrgyzstan), as revealed by high-resolution seismic reflection data. Clim. Past Discuss. http://dx.doi.org/10.5194/cp-2016-3 submitted for publication.
Gibbons, A.B., Megeath, J.D., Pierce, K.L., 1984. Probability of moraine survival in a succession of glacial advances. Geology 12, 327–330.
Gosse, J.C., Phillips, F.M., 2001. Terrestrial in situ cosmogenic nuclides: theory and application. Quat. Sci. Rev. 20, 1475–1560.
Grigina, O.M., Fortuna, A.B., 1981. Paleogeography of the Cenozoic of the Northern Tien Shan (In Russian). Frunze (Bishkek), Ilim, 150 pp.
Grigorienko, P.G., 1970. The Main Features of Geological Development of Krygyz Tien Shan during the Quaternary Period (In Russian), Materials about Cenozoic Geology and the Newest Tectonic of the Tien Shan. Frunze, Ilim.
Hallet, B., Hunter, L., Bogen, J., 1996. Rates of erosion and sediment evacuation by glaciers: a review of field data and their implications. Glob. Planet. Change 12, 213–235.
Hancock, G.S., Anderson, R.S., 2002. Numerical modeling of fluvial strath-terrace formation in response to oscillating climate. Geol. Soc. Am. Bull. 114, 1131–1142.
Herdendorf, C.E., 1990. Distribution of the World's Large Lakes. In: Tilzer, M.M., Serruya, C. (Eds.), Large Lakes. Springer-Verlag, Berlin, pp. 3–38.
Imbrie, J., Hays, J.D., Martinson, D.G., McIntyre, A., Mix, A.C., Morley, J.J., Pisias, N.G., Prell, W.L., Shackleton, N.J., 1984. The orbital theory of Pleistocene climate: support from a revised chronology of the marine delta 18O record. In: Berger, A., Imbrie, J., Hays, J., Kukla, G., Saltzman, B. (Eds.), Milankovitch and Climate, Part I. Reidel, Boston, pp. 269–305.
Kohl, C.P., Nishiizumi, K., 1992. Chemical isolation of quartz for measurement of in situ-produced cosmogenic nuclides. Geochim. Cosmochim. Acta 56, 3583–3587.
Koppes, M., Gillespie, A.R., Burke, R.M., Thompson, S.C., Stone, J., 2008. Late Quaternary glaciation in the Kyrgyz Tien Shan. Quat. Sci. Rev. 27, 846–866.
Leopold, L.B., Bull, W.B., 1979. Base level, aggradation, and grade. Proc. Am. Philos. Soc. 123, 168–202.
Lifton, N., Beel, C., Hättestrand, C., Kassab, C., Rogozhina, I., Heermance, R., et al., 2014a. Constraints on the late Quaternary glacial history of the Inylchek and Sary-Dzaz valleys from in situ cosmogenic 10 Be and 26 Al, eastern Kyrgyz Tian Shan. Quat. Sci. Rev. 101, 77–90.
Lifton, N., Sato, T., Dunai, T.J., 2014b. Scaling in situ cosmogenic nuclide production rates using analytical approximations to atmospheric cosmic-ray fluxes. Earth Planet. Sci. Lett. 386, 149–160.
Lu, H., Burbank, D.W., Li, Y., 2010. Alluvial sequence in the north piedmont of the Chinese Tian Shan over the past 550kyr and its relationship to climate change. Palaeogeogr. Palaeoclimatol. Palaeoecol. 285 (3), 343–353.
Marrero, S.M., Phillips, F.M., Borchers, B., Lifton, N., Aumer, R., Balco, G., 2016. Cosmogenic nuclide systematics and the CRONUScalc program. Quat. Geochronol. 31, 160–187.
Melnikova, A.P., 1986. The History of Development of Vegetation of Northern and Central Tien Shan at Holocene: Synopsis of Thesis of Kandidate on Geographical Science, Frunze, 25pp.
Merritts, D.J., Vincent, K.R., Wohl, E.E., 1994. Long river profiles, tectonism, and eustasy: a guide to interpreting fluvial terraces. J. Geophys. Res. Solid Earth 99, 14031–14050.
Molnar, P., Tapponnier, P., 1975. Cenozoic tectonics of Asia: effects of a continental collision. Science 189 (4201), 419–426.
Molnar, P., Brown, E.T., Burchfiel, B.C., Qidong, D., Xianyue, F., Jun, L., Raisbeck, G.M., Jianbang, S., Zhangming, W., Yiou, F., Huichuan, Y., 1994. Quaternary climate-change and the formation of river terraces across growing anticlines on the north flank of the Tien Shan, China. J. Geol. 102, 583–602.
Muto, T., Swenson, J.B., 2005. Large-scale fluvial grade as a nonequilibrium state in linked depositional systems: theory and experiment. J. Geophys. Res. 110, F03002.
Narama, C., Kondo, R., Tsukamoto, S., Kajiura, T., Ormukov, C., Abdrakhmatov, K., 2007. OSL dating of glacial deposits during the last glacial in the Terskey-Alatoo range, Kyrgyz Republic. Quat. Geochronol. 2, 249–254.

Narama, C., Kondo, R., Tsukamoto, S., Kajiura, T., Duishonakunov, M., Abdrakhmatov, K., 2009. Timing of glacier expansion during the last glacial in the inner tien shan, Kyrgyz Republic by OSL dating. Quat. Int. 199 (1), 147–156.
Pan, B.T., Burbank, D., Wang, Y.X., Wu, G.J., Li, J.J., Guan, Q.Y., 2003. A 900 ky record of strath terrace formation during glacial-interglacial transitions in northwest China. Geology 31, 957–960.
Pazzaglia, F.J., Brandon, M.T., 2001. A fluvial record of long-term steady-state uplift and erosion across the Cascadia forearc high, western Washington State. Am. J. Sci. 301, 385–431.
Pederson, J.L., Anders, M.D., Rittenhour, T.M., Sharp, W.D., Gosse, J.C., Karlstrom, K.E., 2006. Using fill terraces to understand incision rates and evolution of the Colorado River in eastern Grand Canyon, Arizona. J. Geophys. Res. Earth Surf. 111, F02003. http://dx.doi.org/10.1029/2004JF000201.
Personius, S.F., Kelsey, H.M., Grabau, P.C., 1993. Evidence for regional stream aggradation in the central Oregon Coast Range during the Pleistocene-Holocene transition. Quat. Res. 40, 297–308.
Phillips, J.D., 1991. Multiple modes of adjustment in unstable river channel cross-sections. J. Hydrol. 123, 39–49.
Phillips, W.M., McDonald, E.V., Reneau, S.L., Poths, J., 1998. Dating soils and alluvium with cosmogenic Ne-21 depth profiles: case studies from the Pajarito Plateau, New Mexico, USA. Earth Planet. Sci. Lett. 160, 209–223.
Pinter, N., Keller, E.A., West, R.B., 1994. Relative dating of terraces of the Owens River, northern California, and correlation with moraines of the Sierra Nevada. Quat. Res. 42, 266–276.
Pisias, N.G., Moore Jr., T.C., 1981. The evolution of Pleistocene climate: a time series approach. Earth Planet. Sci. Lett. 52 (2), 450–458.
Poisson, B., Avouac, J.P., 2004. Holocene hydrological changes inferred from alluvial stream entrenchment in North Tian Shan (Northwestern China). J. Geol. 112, 231–249.
Porter, S.C., An, Z.S., Zheng, H.B., 1992. Cyclic Quaternary alluviation and terracing in a nonglaciated drainage-basin on the north flank of the Qinling Shan, central China. Quat. Res. 38, 157–169.
Reheis, M.C., Palmquist, R.C., Agard, S.S., Jaworowski, C., Mears Jr., B., Madole, R.F., Nelson, A.R., Osborn, G.D., 1991. Quaternary history of some southern and central Rocky Mountain basins. In: Morrison, R.B. (Ed.), Quaternary Nonglacial Geology: Conterminous U.S.: Boulder, Geological Society of America, the Geology of North America, K-2, pp. 407–440.
Reimer, P.J., Bard, E., Bayliss, A., Beck, J.W., Blackwell, P.G., Ramsey, C.B., et al., 2013. IntCal13 and Marine13 radiocarbon age calibration curves 0–50,000 years cal BP. Radiocarbon 55 (4), 1869–1887.
Ricketts, R.D., Johnson, T.C., Brown, E.T., Rasmussen, K.A., Romanovsky, V.V., 2001. The Holocene paleolimnology of Lake Issyk-Kul, Kyrgyzstan: trace element and stable isotope composition of ostracodes. Palaeogeogr. Palaeoclimatol. Palaeoecol. 176, 207–227.
Romanovsky, V.V., 2002. Water level variations and water balance of Lake Issyk-Kul. In: Klerkx, J., Imanackunov, B. (Eds.), Lake Issyk-Kul: its Natural Environment. Kluwer Academic Publishers, Dordrecht, pp. 45–57.
Ruddiman, W.F., Raymo, M., McIntyre, A., 1986. Matuyama 41,000-year cycles: north Atlantic Ocean and northern hemisphere ice sheets. Earth Planet. Sci. Lett. 80 (1), 117–129.
Selander, J., Oskin, M., Ormukov, C., Abdrakhmatov, K., 2012. Inherited strike-slip faults as an origin for basement-cored uplifts: example of the Kungey and Zailiskey ranges, northern Tian Shan. Tectonics 31, TC4026. http://dx.doi.org/10.1029/2011TC003002.
Stuiver, M., Polach, H.A., 1977. Reporting of $^{14}C$ data: discussion. Radiocarbon 19, 355–363.
Takeuchi, N., Fujita, K., Aizen, V.B., Narama, C., Yokoyama, Y., Okamoto, S., Naoki, K., Kubota, J., 2014. The disappearance of glaciers in the Tien Shan mountains in Central Asia at the end of Pleistocene. Quat. Sci. Rev. 103, 26–33.
Thompson, S.C., 2001. Active tectonics in the central Tien Shan. Kyrgyz Republic [Ph.D. Thesis]. University of Washington, Seattle, 141 pp.
Thompson, S.C., Weldon, R.J., Rubin, C.M., Abdrakhmatov, K., Molnar, P., Berger, G.W., 2002. Late Quaternary slip rates across the central Tien Shan, Kyrgyzstan, central Asia. J. Geophys. Res. Solid Earth 107, 2203.
Trofimov, A.K., 1978. Bottom Relief of Issyk-Kul: Geological basis of Seismic Division of the Issyk-Kul basin (In Russian), pp. 57–66. Frunze Ilim.
Trofimov, A. K., 1990, Quaternary Deposits of Issyk-Kul basin in Connection to its Tectonics: Izvestia a. S. Kirghyzskoy SSR, 1990(1) (In Russian).
Weldon, R.J., 1986. Late Cenozoic Geology of Cajon Pass: Implications for Tectonics and Sedimentation along the San Andreas Fault [Ph.D. thesis]. California Institute of Technology, Pasadena, 400 pp.
Youn, J.H., Seong, Y.B., Choi, J.H., Abdrakhmatov, K., Ormukov, C., 2014. Loess deposits in the northern Kyrgyz Tien Shan: implications for the paleoclimate reconstruction during the late quaternary. Catena 117, 81–93.
Zabirov, R.D., Korotayev, V.N., Nikiforov, L.G., 1973. Some problems of Quaternary history of Issyk-Kul lake. Geomorphology 1973, 63–68 (in Russian).
Zech, R., 2012. A late Pleistocene glacial chronology from the Kitschi-Kurumdu Valley, Tien Shan (Kyrgyzstan), based on 10 Be surface exposure dating. Quat. Res. 77 (2), 281–288.
Zhao, J., Song, Y., King, J.W., Liu, S., Wang, J., Wu, M., 2010. Glacial geomorphology and glacial history of the Muzart River valley, Tianshan range, China. Quat. Sci. Rev. 29 (11), 1453–1463.